PB-225 038

X-RAY FLUORESCENCE SPECTROMETER FOR AIRBORNE PARTICULATE MONITORING

CALIFORNIA UNIVERSITY

PREPARED FOR
ENVIRONMENTAL PROTECTION AGENCY

APRIL 1973

Distributed By:

NTIS
National Technical Information Service
U. S. DEPARTMENT OF COMMERCE

BIBLIOGRAPHIC DATA SHEET	1. Report No. EPA-R2-73-182	2.	PB 225 038

4. Title and Subtitle
X-Ray Fluorescence Spectrometer for Airborne Particulate Monitoring

5. Report Date
April 1973 .

6.

7. Author(s)
F. S. Goulding and J. M. Jaklevic

8. Performing Organization Rept. No.

9. Performing Organization Name and Address
Lawrence Berkeley Laboratory
Berkeley, California 94720

10. Project/Task/Work Unit No.

11. Contract/Grant No.
EPA-IAG-0089(D)/A

12. Sponsoring Organization Name and Address

13. Type of Report & Period Covered
Final Jan.1972-Jan.73

14.

15. Supplementary Notes

16. Abstracts An automated system for determining the elemental composition of ambient air has been developed. Airborne particulate matter is collected on up to 36 membrane filters which are sequentially introduced into the sample stream. The duration for the collection period can be adjusted to range from 1 to 24 hours. In the analysis station the elemental composition of the collected particulate matter is determined using an energy dispersive X-ray spectrometer. Each filter is separately analyzed using each of three secondary fluorescers in order to optimize the sensitivity for a wide range of elements which have atomic numbers greater than 12. After a brief analysis period the results for each filter are printed out on a teletypewriter and written on magnetic tape. Up to 36 filters can be accommodated without operator attention.

17. Key Words and Document Analysis. 17a. Descriptors
Airborne particulate monitor
X-ray fluorescence
X-ray tubes
Trace element analysis
Air Sampling

17b. Identifiers/Open-Ended Terms

17c. COSATI Field/Group

Reproduced by
NATIONAL TECHNICAL INFORMATION SERVICE
U S Department of Commerce
Springfield VA 22151

18. Availability Statement Approved for public release, distribution unlimited	19. Security Class (This Report) UNCLASSIFIED	21. No. of Pages ~~70~~ 69
	20. Security Class (This Page) UNCLASSIFIED	22. Price ~~$3.50~~ -145

EPA-R2-73-182

319043

X-RAY FLUORESCENCE SPECTROMETER FOR AIRBORNE PARTICULATE MONITORING

by

Fred S. Goulding and Joseph M. Jaklevic

Lawrence Berkeley Laboratory
Berkeley, California 94720

Interagency Agreement No. EPA-IAG-0089(D)/A
Program Element No. 1A1003

EPA Project Officers: Robert K. Stevens and Thomas G. Dzubay

Chemistry and Physics Laboratory
National Environmental Research Center
Research Triangle Park, North Carolina 27711

Prepared for

OFFICE OF RESEARCH AND MONITORING
U.S. ENVIRONMENTAL PROTECTION AGENCY
WASHINGTON, D.C. 20460

April 1973

ia

This report has been reviewed by the Environmental Protection Agency and approved for publication. Approval does not signify that the contents necessarily reflect the views and policies of the Agency, nor does mention of trade names or commercial products constitute endorsement or recommendation for use.

TABLE OF CONTENTS

SUMMARY 1

1. INTRODUCTION 2

2. MONITORING SYSTEM DESIGN 3

   A. Filter Specifications 3

   B. Range of Elements Measured 3

   C. Data Processing 5

   D. Sampling Station 6

3. ANALYSIS STATION 7

   A. Semiconductor Detector Spectrometer and Associated Electronics 7

   B. Mechanical Design 8

   C. X-ray Tube - Fluorescer - Detector Geometry 9

   D. Sample Changer 10

4. CONTROL ELECTRONICS 10

   A. Dead Time Correction 10

   B. X-ray Tube Power Supply and Controller 12

   C. Data Processing 12

5. EXPERIMENTAL RESULTS 24

   A. Calibration 24

   B. Sensitivity 32

   C. Particle Size and Matrix Effects 34

6. CONCLUSIONS 37

REFERENCES 37

TABLE CAPTIONS 38

FIGURE CAPTIONS 38

APPENDIX A.1

X-RAY FLUORESCENCE SPECTROMETER FOR AIRBORNE PARTICULATE MONITORING

Fred S. Goulding and Joseph M. Jaklevic

Lawrence Berkeley Laboratory
University of California
Berkeley, California 94720

SUMMARY

The purpose of this contract was to develop an elemental monitoring system for air particulates based on analysis by an energy-dispersive X-ray spectrometer. The program has included the development of a carrier for cellulose filters (that are relatively free of trace metals), of an automatic sampling station to expose these filters to known amounts of air, and of a fully automatic analysis system capable of analyzing for most of the important elements at levels in the 10 ng/cm^2 range in the filters. The basic design of the system has been described in earlier progress reports, and particularly in the first one (see Appendix I). This final report will mainly discuss experimental results achieved during the final system testing, but any modification made in this phase of the work will also be detailed.

Final assembly and testing of both the sampling and analysis station have been completed and the units shipped to EPA at Research Triangle Park, North Carolina. There the system has been reassembled, tested, and calibrated by LBL personnel.

Virtually all of the design objectives outlined in previous reports have been achieved. Recent modifications to the hardware and computer programs to accommodate the automatic sequencing of three fluorescer targets were successfully completed. An extensive program of testing for accuracy and stability has been carried out and the results of the calibration have been validated by comparison with known standards. The analysis accuracy and the detectable limits achieved are within previous predictions for most elements; no significant drift or unstability in the calibration has been observed.

1. INTRODUCTION

Previous reports have described various components of the LBL aerosol particulate analysis system and the progress made in assembling the complete system. The spectrometer has now been completed, tested, and delivered to the EPA. During this final interval no important changes were made in the basic design. Hardware changes have been limited to engineering refinements indicated by extensive testing in the study of particulates at Pasadena during October and November. The major effort in the last period has been devoted to extending the capabilities of the computer program to include the three fluorescent energies, and to developing and testing the final data analysis program. An extensive experimental program designed to evaluate the performance of this system and validate the analytical results has been completed.

Since the basic design remains unchanged, the emphasis of this final report will be on the experimental results obtained in the final stages and their relationship to system performance. Where necessary, a brief review of design details discussed in previous reports will be included. Documents containing more detailed engineering data and an operator's manual are in the process of being prepared.

2. MONITORING SYSTEM DESIGN

A. Filter Specifications

No changes have been made in the filter holder. The samples consist of 2" x 2" plastic sample holders containing 37 mm diameter filters. Mechanisms in the air sampler and X-ray fluorescence unit are designed to manipulate and accurately position these samples. The 37 mm diameter was chosen as the optimum size consistent with availability of suitable filters--both Millipore and Nucleopore filter substrates are available in these sizes. Cellulose filters can also be cut to this diameter.

Distortion of filters by cold flow of the plastic holder caused by careless storage has caused some problems but appears to be easily corrected. Filter holders can be returned to their original shape by pressing between two plates heated to 50°C; subsequent storing in a tightly packed box retains this shape.

A supply of 200 holders with mounted 0.8 μ Millipore filters have been delivered to EPA. In addition, 1000 blank filter holders have been delivered together with the jig used to glue filters to the holders. These should be adequate to support an initial experimental program by EPA personnel.

B. Range of Elements Measured

The range of elements measured in the completed system is the same as that described in an earlier progress report. For convenience, this list (Table 1) is repeated here together with the X-ray absorption edge energies and the energies of the principal emission lines.[1]

TABLE 1. Elements Included In Analysis

ELEMENT	ATOMIC NO.	K BINDING ENERGY[a)]	Kα ENERGY[a)]	Kβ ENERGY[a)]
Al	13	1.559	1.486	-
Si	14	1.838	1.739	-
P	15	2.142	2.013	-
S	16	2.470	2.307	-
Cl	17	2.819	2.621	-
K	19	3.607	3.312	3.590
Ca	20	4.038	3.690	4.012
Ti	22	4.964	4.508	4.931
V	23	5.463	4.949	5.426
Cr	24	5.988	5.411	5.946
Mn	25	6.537	5.894	5.489
Fe	26	7.111	6.398	7.058
Co	27	7.709	6.924	7.648
Ni	28	8.331	7.471	8.263
Cu	29	8.980	8.040	8.904
Zn	30	9.660	8.630	9.57
Ga	31	10.368	9.241	10.26
As	33	11.863	10.53	11.72
Se	34	12.652	11.21	12.49
Br	35	13.475	11.91	13.29
Rb	37	15.201	13.73	14.96
Sr	38	16.106	14.14	15.83
Zr	40	18.00	15.7	17.7
Nb	41	18.99	16.6	18.7
Mo	42	20.00	17.4	19.6
Cd	48	26.71	23.1	26.2
In	49	27.93	24.1	27.2
Sn	50	29.19	25.2	28.4
Sb	51	30.49	26.3	29.7
I	53	33.16	28.5	32.2
Ba	56	37.40	32.1	36.3

ELEMENT	ATOMIC NO.	L BINDING ENERGY[b)]	$L\alpha_1$ ENERGY	$L\beta_1$ ENERGY
Hg	80	14.21	9.99	11.82
Pb	82	15.21	10.55	12.61

a) Ref. 6. Energies are in keV. For heavier elements the energies are averages of the partially resolved times.

b) The L shell binding energy quoted is the L_{II} shell.

The choice of secondary targets has been changed slightly since earlier reports. Cu, Mo and Tb have now been chosen as a reasonable compromise between uniform analytical sensitivity over a wide range of atomic numbers (Z) and availability of pure materials. The energies of the principal lines for these targets are 8.0 keV, 17.4 keV and 44.0 keV respectively. The probability of excitation for a given element depends strongly upon the difference between excitation energy and the X-ray absorption edge. Using these three excitation energies, the calculated relative probabilities for characteristic X-ray generation are as shown in Figure 1. The data represents cross sections for equivalent photon flux using each of the three targets. Each curve gives the Z dependence of the yield for a given secondary target--the abrupt cut-off at high energies represents the K-shell ionization threshold. Since the characteristic X-ray yield converts directly into analytical sensitivity, the reason for the choice of the three fluorescers becomes apparent.

C. Data Processing

No major changes in the data processing system have occurred. The hardware consists of a TI960A computer interfaced directly to the X-ray analyzer for control functions, and to a Northern Scientific 1024 Channel ADC for data acquisition. Input/output to the computer is accomplished either via teletype or IBM compatible magnetic tape. In addition, there are a certain number of computer functions which can be controlled by means of a hard-wired control panel. The total memory capability of the computer has now been increased from 12,000 to 16,000 16-bit words in order to adequately handle the three fluorescers.

To facilitate program development we have written an assembler operating in the LBL CDC 6600/7600 central computer system. This has enabled us to assemble programs on these computers which generate program magnetic tapes that can be loaded directly into the TI960A computer. The use of this assembly language has greatly facilitated program development in the later stages and will continue to be useful for future program development.

D. Sampling Station

No basic changes have been made in the sampling station design in recent months. The schematic of Figure 2 shows the basic elements. Minor modifications of the sequencer module were implemented in order to increase the electronic noise immunity of the control logic. A continuous testing program has indicated that the unit operates reliably over long periods.

The air sampler has been calibrated in a series of measurements in which the output flow rate has been measured for a number of filters and compared with flow estimates based upon filter area and pressure differential. It is important to determine the effective area of the filter so that numbers obtained from the X-ray fluorescence analyzer, which are expressed in ng/cm^2 of elemental impurities on the filter, can be converted into ng/m^3 of the air sampled.

The air flow through the filters was 52.72 l/min as measured by a compensated displacement gas meter. The average pressure differential across the filter in these tests was 11.5 inches of Hg. By observing the density profile of particulates on a number of exposed filters it was determined that the effective area of the filter in the sampling system was 7.96 cm^2, and that a gradual decrease in deposition of particulates occurs

over the outer 1.7 mm of the periphery of the opening in the filter holder. These results are consistent with the published Δp vs. velocity relationship for 0.8 μ Millipore filters. For Δp = 11.5" Hg, the air velocity is 109.3 cm/sec, and, assuming an effective area of 8.00 cm^2, the conversion factor (based on measured flow rate or measured pressure drop) is 1 ng/cm^2 of filter = 1.265 ng/m^3 of air for a two-hour air sample. This conversion factor holds only for 0.8 μ Millipore filters. For other types of filters or pore sizes, the conversion factor can be calculated from the pressure differential if the Δp vs. velocity characteristic for the filter are known.

3. ANALYSIS STATION

A. Semiconductor Detector Spectrometer and Associated Electronics

Details of the X-ray spectrometer system have been extensively documented elsewhere.[2,3] The guard-ring detector is 6 mm in diameter and 3 mm thick. Its energy resolution is 135 eV FWHM on a pulser and 185 eV FWHM on 5.9 keV X-rays. Some idea of the resolution of the system for various X-ray lines can be obtained by consulting Figure 3 in conjunction with the data of Table 1. The energy dependence of resolution for the EPA system can be obtained by interpolating a curve between those corresponding to electronic resolutions of 100 eV and 150 eV. Scanning measurements performed after the assembly of the detector in the vacuum cryostat indicate that the detector is within 0.2 mm of the axis of the cryostat enclosure and its face is 4.5 mm from the front surface of the cap. Accuracy in alignment is important since positioning of the collimators, sample, and fluorescer targets are all referred to this center-

line. This alignment can only be measured after the system has been assembled, pumped, and cooled to 90°K since the relative contraction of various members can result in dimensional changes of several millimeters.

The efficiency of the detector was calculated using data based on previous measurements of detector window thicknesses and a compilation of X-ray absorption cross sections.[4] These data are summarized in Figure 4. Each of the individual curves represents the effect of that particular component on the relative efficiency. For example, the combined effect of 0.001" Be and 2 cm air would be the product of the two curves shown. The existing system can operate either with helium or air; the intrinsic detector window and 25 μ Be are always present. More recent measurements on high-energy X-ray yields indicate that the roll-off of efficiency at higher energies is somewhat more rapid than indicated in these curves. This is believed to be due to fringing effects around the periphery of the detector and can start to affect the efficiency at energies as low as 10 keV. The effects become important in the later discussion concerning the calibration for higher energies.

B. Mechanical Design

The X-ray tube-fluorescer and detector assembly has been shielded with aluminum-lined lead absorbers to keep radiation exposure to people in the area well below tolerable limits. Measurements performed with and without the shielding have established that virtually no additional background is caused in the measured X-ray spectrum by the Al-lined shields. The

shielding, together with electrical interlocks on access doors are designed to ensure safe operation. The maximum radiation level occurs when the tube is operating at 75 keV and 400 μA--at the outside surface of the cabinet it is less than 5 mr/hr at all points.

C. X-ray Tube - Fluorescer - Detector Geometry

No basic changes in design have been implimented in the final period. However, a new X-ray tube has been installed and the secondary targets and fluorescer changer design has been improved. Figure 5 is a cross section showing the final tube-fluorescer-detector geometry. Extensive measurements were performed to optimize X-ray intensity and peak/background of the exciting radiation. These included measurements of the electron beam spot size on the tube anode using X-ray photographic techniques, and emission vs. anode voltage curves to establish cathode excitation efficiency. Upon achieving maximum beam on target in the tube, the complete geometry was then adjusted to yield maximum counting rate. Measurement of spectra obtained without samples in position were used to evaluate peak/background ratios and to inspect for spurious lines. Additional X-ray transmission filters were inserted at crucial points to reduce scattered background to a minimum. It was found necessary to redesign the collimator to include an additional shield to absorb X-rays that could strike the inner collimator surface directly from the tube anode. Finally, the diameter of the collimator was chosen to allow the detector to view as large an area of the filter as possible without introducing excessive scattering from the sample holder frame. In the final system, the area analyzed on the filter is a slightly elliptical region with a major axis of 3 cm.

D. Sample Changer

With the exception of minor modifications designed to eliminate occasional mechanical failures, the only modification performed on the sample changer involved the incorporation of a helium atmosphere in the void between sample and detector. By placing baffles in appropriate places we maintain an enclosed volume beneath the air filter sample into which helium is continuously introduced via a channel in the shielding. This reduces X-ray absorption in the path between sample and detector. While the use of helium is optional for all three fluorescent energies, maximum benefit results when using the Cu target.

Operator access to the sample stack-loader is provided through a shielded door which is interlocked to stop X-ray output when opened. The control program recognizes the "door-open" condition and restarts the analysis of the sample being analyzed when the door is closed. This permits the insertion of samples at any time during an analysis sequence.

4. CONTROL ELECTRONICS

A. Dead Time Correction

Only minor modifications to the control system have been made in this period to facilitate more convenient manual operation. The fact that widely varying counting rates are produced for various samples and fluorescer targets makes accurate correction for events rejected by the pulse pile up rejector essential if absolute values of elemental concentrations are to be obtained. This correction is achieved by automatically extending the

counting time by a factor which just compensates for the fraction of the total counts rejected by the pile-up rejector. To accomplish this, the timer is designed to measure live time--that is the clock pulses are routed through an electronic gate which is closed for an adjustable period each time a pulse is processed by the detector electronics. Adjustment of this period--set by an adjustable one-shot in the timer--is an essential prerequisite if accurate analysis is to be performed.

The association between counting losses and system dead time is illustrated in Figure 6. This plot of input vs. output rate for a series of different pulse dead times assumes that an ideal pile-up rejector circuit is inhibiting the analysis of any pulses which occur close enough in time to cause false energy information. The roll-off of output rate with increasing input rate is a fundamental limitation of counting experiments and can be serious for large dead times such as are used in the X-ray spectrometer system (17 μs in the existing instrument). Thus, at 10,000 counts/second input rate, only 65% of the pulses are ultimately stored.

The dead-time corrector used in the live time clock was adjusted by requiring that the accumulated counts due to a peak produced by a radioisotope source remained constant as the X-ray tube flux was varied to give a wide range of total counting rates. After final adjustment, the counting rate in the radioisotope peak was found to vary by 0.5% from 500 cts/sec to 10^4 cts/sec (35% dead time) and 2.5% from 500 cts/sec to 2×10^4 cts/sec (65% dead time). The maximum counting rates obtained in our experience with air filter samples is 10^4 cts/sec while operating the X-ray tube at 45 kV and 400 μA with the molybdenum target.

B. X-Ray Tube Power Supply And Controller

The X-ray tube controller and high voltage supply have been thoroughly checked out at voltages up to 80 keV. The final settings of the preset voltage and emission current conditions for each of the three fluorescers are as follows: a) Cu, 35 keV, 400 μA, b) Mo, 50 keV, 400 μA and c) Tb, 75 keV, 400 μA. These can easily be changed to accommodate conditions which might occur with different samples. Reproducibility of the settings appears to be within a few percent; including any possible long term drifts the currents and voltages should remain within 5% of their preset values.

C. Data Processing

This final period, has been dominated by computer programming for control and spectral data processing, and by testing the operation of the programs. The following discussion will be divided into three sections 1) control and routine monitoring functions, 2) spectrum analysis 3) calibration and output. We will describe the operation of the programs in some detail. Validation of the results is described in the section on experimental studies.

1. Control and Routine Monitoring Programs:

The analysis system is controlled by the computer in its normal mode of operation. Once a sequence of secondary fluorescers and the running time of each has been selected on the sequencer and timer units, the operator is only required to load samples in the input stack then push the "START" button on the computer. The samples are

automatically loaded in sequence and the appropriate data taken from each analysis. The spectral data is stored during the analysis period; at the end of that time, the spectrum is written on magnetic tape, the data are analyzed and the results (in ng/cm^2) are printed on the teletype and written on magnetic tape. After the last sample has been analyzed, the system returns to a standby condition to await the next batch of samples.

In addition to the fully automatic mode of operation, the sequence of steps can be controlled manually. A keyboard on the computer control unit permits the operation of the computer as a pulse height analyzer and operations such as "START ADC", "CLEAR MEMORY", "DISPLAY DATA", and "WRITE or READ MAGNETIC TAPE" can all be performed by pushing appropriate buttons. These features are used mainly during the set-up and calibration period although the versatility afforded by these options is also useful in other situations.

In addition to executing these sequencial steps, the computer also periodically monitors various key parameters of the analysis system in order to inform the operator via teletype message of any malfunctions. Some problems are considered serious enough to automatically shut down the system and await corrective action by the operator, whereas, in other cases, it is considered adequate to inform the operator that some condition exists.

A partial list of messages programmed into the computer are listed on the following page.

Computer Messages:

FRONT SHIELD OPEN PROGRAM STOPPED

SAFETY INTERLOCKS DEFEATED PROCEED WITH CAUTION

BACK DOOR OPENED

NO EMISSION FROM XRAY TUBE

XRAY TUBE OVER HEATED

HIGH VOLTAGE SUPPLY FAILURE

SAMPLE CHANGER STUCK

FLUORESCER CHANGER STUCK

LIQUID NITROGEN LEVEL LOW

The program is designed to be as communicative as possible so that an experienced operator can recognize most malfunctions and make appropriate responses without consulting operating manuals and trouble-shooting guides. Our experience in testing the control program has been that we were reasonably successful in achieving this goal.

2. Spectrum Analysis:

Crucial to the problem of converting a measured counting rate into a elemental concentration is the extraction of an accurate peak area from the pulse-height spectrum. Since the energy resolution capabilities of the Si(Li) detector does not prohibit some interference of peaks from neighboring elements in the periodic table, it is necessary to accurately subtract out the lines produced by each element so that the value for an adjacent element is not affected. This is a problem

that has received much attention in nuclear counting experiments. Generalized formalisms exist for extracting the deconvoluted data from extremely complex pulse-height spectra. Although one might argue that X-ray fluorescence spectra are much more densely packed with peaks, and hence more difficult to analyze, there are certain reasonable assumptions which can be made regarding X-ray spectra which greatly simplify the problem. Specifically, the number of possible lines in a spectrum is limited and the energies and relative intensities of the lines from any one element are known beforehand. Thus, to a good approximation (virtually exact for air filters) the only free parameters in the problem are the magnitude and shape of the background under the peaks and the relative intensity (concentration) for each of the constituent elements.

When analyzing a series of air samples acquired on the same filter material, the continuous background due to scattering from the matrix (filter substrate) is similar from sample to sample. Furthermore, the variation in background due to varying matrix contributions is mainly one of relative magnitude (rather than shape) provided the average Z of the matrix remains unchanged--as is the case for filter media which are predominantly hydrocarbons.

We have taken advantage of this fact by using for the background shape a spectrum acquired by analyzing a blank air filter of the type used for particulate collection. This has the advantage that any trace impurities arising either from the filter medium or caused by the analysis system itself, are automatically excluded from analysis. Tests

performed on heavily loaded filters showed that the background contribution could be accurately subtracted out over almost all the energy range covered by the spectrum by normalizing the blank filter spectrum to the unknown spectrum just over the region containing the coherent and incoherent scatter peaks of the exciting radiation. This is valid since the scattered radiation is dominated by the matrix as long as the filter loading does not appreciably change the average Z of the sample.

Calculation of the areas of the X-ray peaks is potentially a more difficult problem due to the variation in relative intensities of the elements and the possibility of interferences from spectral lines. The usual approach to this problem is to mathematically generate a function which simulates the response of the system to a particular photon energy. The shape is then fitted to the experimental data, usually by a least squares method, and the peak location and area determined. As noted earlier the peak location for X-rays is fixed; furthermore, the complexity of the X-ray lines, both in terms of $K\alpha/K\beta$ ratios and in regard to partially-resolved $K\alpha_1$, $K\alpha_2$ lines makes the synthesis of such line shapes difficult. Fortunately, the profile of the instrumental response to the X-rays of an element can be established by running a spectrum from a pure sample of the element. We have taken advantage of this by using a stored spectrum of the instrumental response to the X-rays of an element as a shape standard for that element. Thus the problem of determining the area of a given peak reduces to that of comparing the intensity of the unknown peak to that of a stored shape-standard spectrum. Once this intensity ratio has been established, the total contribution of that element to the spectrum, including all X-ray lines, can be subtracted from the spectrum.

Figure 7 illustrates the operation of the program on a schematic spectrum as shown in the upper left hand portion of the figure. The blank filter spectrum is first compared to the unknown sample over the specified shaded region, normalized, and then subtracted point by point to give the STEP #2 spectrum. The lines due to elements #1, #2, etc. are then sequentially stripped out after first comparing intensities over the shaded regions to derive normalizing factors. Any selected portion of a spectrum can be specified for comparison--this is necessary when considering more complex spectra where regions with overlapping lines must be avoided in making the comparison. After subtraction of the last elements, the residual counts in the spectrum should be zero within statistics.

In practice, the problem is slightly more complicated. Samples used for generating shape standards must be made of material sufficiently thin to prevent changes in the $K\alpha/K\beta$ ratio due to self-absorption. Also, to ensure that interference effects between elements are minimal, it is necessary to carefully choose the order in which elements are removed from the spectrum. (For example Pb before As, Fe before Co, etc.) In the present program, the sequence of removal of elements is specified by including each element in one of three groups. These three groups are analyzed in order, but the elements within a group are removed from the spectrum in order of decreasing intensity. In the above case, Pb and Fe might be in group 1 while As and Co could be in groups 2 or 3. This presupposes some knowledge of possible interferences on the part of the person specifying the order. Other features

of the program include a peak-shifting routine to correct for any small shifts in peak location which might have occurred between the time that the shape standards were stored and that when the unknown spectrum was run. Our present experience indicates that the stability of the system when running continuously is adequate to use the same shape standards for several weeks of running.

The ultimate test of any such program lies in its ability to reproducibly calculate the correct answer. Table 2 is a summary of measurements performed on spectra acquired in 11 sequential analyses of the same air filter. Each analysis consisted of a separate data-taking interval with the acquired spectrum being analyzed using the described program. The entries in the table include the areas calculated by the program, the RMS deviation of the 11 measurements, the mean deviation of the 11 measurements, and the RMS deviation (variance) for any one measurement calcualted from the equation:

$$\text{Variance} = \sqrt{\text{Peak Area} + \text{Background}}$$

The good agreement between the statistical variance (calculated) and the RMS deviation in the experimental results shows that there are no extraneous or systematic program errors. The average ratio of MEAN/RMS for the measured numbers is 0.82; for a Poisson distribution this ratio should be $2/\pi = 0.799$. This supports the conclusion that the variations are purely statistical.

TABLE 2.

Reproducibility of Areas Calculated With Computer Program

ELEMENT	Ca	Ti	Mn	Fe	Cu	Zn	Br	Pb
Mean Area Calculated From 11 Measurements	1244	424	281	11584	5175	3102	9727	14243
RMS Deviation (Measured)	65	49	27	184	115	65	182	173
Mean Deviation (Measured)	54	40	25	144	98	50	137	140
RMS Calculated from Areas (Theoretical)	89	58	48	130	120	85	217	162
Ratio Mean/RMS (Measured)	0.83	0.81	0.93	0.78	0.85	0.77	0.75	0.81

3. Calibration and Data Output:

The program elements which we loosely term "Calibration" contain portions of both the control and peak analysis programs. We refer to that portion of the program with which the operator interacts initially to enter into the computer the necessary data for complete analysis of the acquired spectra.

In the CALIBRATION mode, the program will automatically sequence and accumulate data from a preselected set of samples containing prepared mixtures of elements to be used as shape standards. The elements included in each sample are chosen so as to avoid interelement interferences. In the present arrangement, ten samples are used to cover the 33 elements listed in Table 1. In the same sequence the computer

will accumulate background spectra on a blank for each of the secondary fluorescer energies. Since this process of analyzing shape standards and background is completely automatic, it can be performed overnight without operator attention.

When the sequence is finished the operator enters the additional data required by the analysis program by using a subroutine called from the control panel. This routine asks the operator a series of questions which must be answered for identification of components of the spectral features associated with each element. Figure 8 is a typical K X-ray spectrum with the relevant regions labeled. PRIMARY PEAK is the peak whose area is calculated as a measure of the intensity of the particular element. It is usually the Kα for light elements and either the Lα or Lβ for heavy elements. SECONDARY REGION is any other region to be subtracted out of the spectrum when this element is stripped from it, subject to the same normalization conditions as for the primary peak. A TERTIARY REGION can also be specified to allow for features such as Si X-ray escape peak for light elements or multiple L lines for heavy elements. The FIT REGION is the region of the peak which will be compared to the unknown spectrum in order to establish a normalization factor. It is chosen for maximum statistical significance while avoiding the possibility of overlapping with lines of other elements in the sample. The PEAK CHANNEL is required as identification of the peak to determine the sequence in which the elements are stripped from the spectrum. The regions are specified by the operator responding to the questions asked by the computer by setting a display marker at the lower limit of the region and by then typing in the width (in channels) of the region.

The data regarding relative X-ray excitation efficiency and analysis sequence group are also entered during this calibration phase. The X-ray efficiency factor is used to convert the peak area to ng/cm^2 in the final stage of the data analysis.

The series of questions asked by the computer and some typical responses are as follows:

ELEMENT .....FE	(or any other listed in Table 1)
TO SKIP AN ENTRY, TYPE COMMA	
SET MARKER AT BOTTOM, TYPE CHANNELS IN REGION	
PRIMARY PEAK.....22	(Kα peak)
SECONDARY REGION....20	(Kβ peak)
TERTIARY REGION.....15	(e.g. Si escape peak)
FIT REGION..... 8	
MARK PEAK, HIT CARRIAGE RETURN	(peak channel specified)
F = ...835	(relative X-ray efficiency)
ANALYSIS GROUP (0-8).....2	(specifies group in which element will be subtracted out: 0-2 Cu target 3-5 Mo target 6-8 Tb target

The next element in the standard spectra is then displayed by the operator and the process steps repeated until the necessary information has been initiated for all elements of interest. Following this, analysis regions are specified for each of the three background spectra--the program is then capable of analyzing an unknown spectrum for the elements entered.

The only other data required to convert the peak areas to ng/cm^2 is the normalization factor which multiplies the relative intensities

of the elements by a number which takes into account the data acquisition interval, X-ray tube current, etc. This number is determined by analyzing a known single-element intensity standard under the same conditions as the filters. The answer given by the computer analysis of this standard using a "dummy" normalization factor of unity is then divided by its known concentration to give the proper system normalization factor which is then entered into the program. Periodic analysis of the intensity standard serves as a check on the continued accuracy of the calibration.

Although this procedure may appear somewhat time consuming, it can be completed in two to three hours of operator time for all fluorescers and targets and need only be repeated every several weeks at the most.

Table 3 gives the results of the analysis of a typical urban aerosol sample in the output format generated by the program. The elements are listed in the order in which they were stripped from the spectrum. (A later version of the program will deposit the results in an output buffer and the output will be generated in a standard order.) The column entries are:

a) total peak area

b) area of the background under peak (FWHM)

c) calculated concentration in ng/cm^2 averaged over the filter area

d) statistical error in ng/cm^2 (this does not take into account any other sources of error).

The speed of analysis of a spectrum is limited by the time required to type the results. Table 3 was typed out in about 50 seconds, spectral analysis being achieved while typing was in progress.

TABLE 3. Computer Output Of Results

	PK INTEGRAL	BKGD INT.	NGM/SQ CM	+ -
PB	22539	6599	1466	12
BR	15385	1694	466	5
FE	7535	1747	739	10
CA	1525	1783	595	23
K	2312	3539	1162	39
TI	306	1054	74	10
CU	381	2817	22	5
SE	223	1315	7	2
V	149	1178	28	8
AS	805	1348	28	3
CO	0	980	0	4
RB	26	4279	0	3
ZN	1082	1649	53	4
SR	485	11813	13	4
CR	365	1146	53	6
NI	244	994	15	3
MN	250	1121	31	5

5. EXPERIMENTAL RESULTS

A. Calibration:

Before proceeding with the details of the experimental tests of the calibrated instrument, a few brief remarks concerning the theoretical basis for the method are given.

The theoretical equation for the intensity (I_i) of an X-ray line of element i for the case of a homogeneous sample of thickness d irradiated with photons of energy E_o and incident flux I_o is given in Figure 9. This expression is derived by integrating the absorption cross section for the incident X-rays and the escape probability for the fluorescent X-ray over the thickness of the sample. For the case of very thin specimens (such as air filters), the expression in brackets reduces to unity, and the equation simplifies to:

$$I_i = [I_o G] [\tau_i \omega^i_{K,L} \varepsilon_i] \rho_i d \qquad (1)$$

where G includes all geometry factors, τ_i is the photoelectron cross section for the i^{th} element at energy E_o, $\omega^i_{K,L}$ is the K,L shell fluorescence yield,[5] ε_i is the intrinsic detector efficiency for photons of energy E_i, and ρ_i d is the concentration of the element in gm/cm^2. The first bracketted term is independent of which element is being analyzed and represents a total normalizing factor which we call 1/N. The second term is specific to the element i and represents a selective K or L X-ray excitation cross section which we call F_i--these are the quantities plotted from theory in Figure 1. The concentration of any element is then expressed simply as:

$$\rho_i = \frac{I_i}{F_i} N \qquad (2)$$

The F_i and N are now recognized as the relative excitation efficiency and normalizing factor referred to in the previous section of this report describing the computer program. Obviously the most critical part of calibration is obtaining the proper values for F_i. Although reasonable values for the quantities of interest are available in the literature, there are certain assumptions inherent in the derivation of the equation which are not rigoriously satisfied in practice. However, the theoretical values do tell us that the total yield is a simple well-behaved function of Z. With this modest assumption it is possible to generate a complete calibration curve by measuring the relative F_i for a series of elements and assume that data can be interpolated between measured values subject to the constraints imposed by the theoretical equation.

We have performed such a set of measurements using a series of evaporated thin film samples of known concentration in $\mu g/cm^2$. Where convenient films were not available, we have used compounds with known ratios of elements to give data for regions not otherwise covered in the study. One consequence of these measurements was the discovery that the relative efficiencies shown in Figure 1 did not take adequate account of the reduction in detection efficiency at higher energies--particularly with reference to the fringing effects around the periphery of the detector. After applying this correction to the theoretical factors, the results shown in Table 4 were obtained. The excellent agreement between the standard concentrations and the measured values demonstrates that the system is capable of accurate calibration for single element standards. Further validation was obtained from analysis of chemical compounds in which the relative concentration of elements was well known

TABLE 4. Comparison of Measured Concentration of Standard Samples

ELEMENT	FLUORESCER	MEASURED DENSITY[a] ($\mu g/cm^2$)	ACCEPTED VALUE[b] ($\mu g/cm^2$)
Al	Cu	1550 c)	2200 d)
Si	Cu	2380	2430 d)
S	Cu	2820	2970 d)
Ti	Cu	90	101
Cr	Cu	117	122
Fe	Cu	83 e)	83
Ti	Mo	100	101
Cr	Mo	121	120
Fe	Mo	94	87
Ni	Mo	109	100
Cu	Mo	55	49
Pb	Mo	132	131
Zr	Tb	66	61 f)
Pd	Tb	138	142
Cd	Tb	92	93 f)
Sn	Tb	142	138
Ba	Tb	122	124 f)

a) Statistical errors are less than 1% in all cases of evaporated films.

b) Thicknesses of evaporated films were determined by weighing. Estimated errors are <5%.

c) The discrepancy in this comparison could easily be due to heavy elements in the 1100 Al alloy used.

d) These densities represent the effective weight of infinitely thick samples.

e) The Cu fluorescer comparisons are normalized to the Fe value.

f) These were obtained by using samples of $ZrBr_4$, $CdBr_2$, and $BaBr_2$; the Br intensity was measured with the Mo fluorescer.

(e.g., Ba Cr O_4, Pb Cr O_4, K Mn O_4, etc.). Measurements performed over a period of two weeks indicated that the calibration was stable to within 3% over this interval.

Figure 10 is a plot of the above data showing the interpolation curves used for elements not included in Table 4. The F_i values used in the final analysis program were taken from these curves. Comparison of Figure 10 with Figure 1 shows the effect of the reduced detector efficiency at higher X-ray energies.

Analysis of more complex samples, such as air filters, involves additional considerations such as interference between spectral lines from two elements, particle size and matrix effects. Spectral-line interference is a property common to all energy-dispersive X-ray fluorescence analysis systems and will be treated independently from the questions of particle size and matrix effects which are inherent in any X-ray fluorescence method, and which become serious problems in calibration for light elements.

The degree to which the complex spectrum can be accurately reduced into its constituent characteristic X-rays depends mostly upon the sophistication of the peak analysis program. The ultimate limits of accuracy of such spectral analysis are set by counting statistics--accuracies for individual elements depend upon the relative magnitudes of any possible interfering lines. Some idea of the effect on sensitivity produced by spectral-line interference can be obtained by considering a typical case of interference--the Fe Kβ/Co Kα overlap. Let the Fe Kβ/Kα ratio be R, the rms deviation in a concentration measurement N be σ, and the number of background counts under a peak in the Fe-Co energy region be N_B.

Then:

$$\sigma^2(Fe) = N_{Fe} + N_B$$

$$\sigma^2(Co) = N_{Co} + N_B + R\,(N_{Fe} + N_B)$$

where N_{Fe}, N_{Co}, N_B are the number of counts in the iron Kα peak, cobalt Kα peak, and background (assumed constant) respectively. The value of R is about 0.2, so

$$\sigma^2(Co) = N_{Co} + 1.2\,N_B + 0.2\,N_{Fe}$$

(the detectable limit for Co is now a function of the concentration of iron). For a large iron concentration, this equation becomes

$$\sigma^2(Co) = 0.2\,N_{Fe}$$

or $$3\sigma\,(Co) = 1.5\,\sigma\,(Fe)$$

In other words, the detection limit for cobalt in the case of high iron concentration is about 1.5 times the variance in the iron concentration determination.

Table 5 is a tabulation of data showing the 3σ detectability limit for Co as a function of Fe concentration. The values for N_B, N_{Fe} and N_{Co} are based on experimental measurements.

TABLE 5.

Detectibility of Co as a Function of Fe Concentration
for 5 Minute Counting Interval

Fe Concentration (ng/cm^2)	N_{Fe}	N_B	Co Detectibility (ng/cm^2) [a]
0	0	1.75×10	9.1
10	1.5×10^2	"	9.2
10^2	1.5×10^3	"	9.6
10^3	1.5×10^4	"	14.1
10^4	1.5×10^5	"	35
10^5	1.5×10^6	"	109

a) Defined as 3σ of the background.

The most meaningful judgement of accuracy in multiple element analysis is to apply the program to real samples and compare the results with independent measurements. Table 6 presents a comparison of results obtained using the complete system on spectra obtained using Mo excitation which is generally the most complex. The data are the results of analysis of eight separate air filter samples with widely varying loadings. They are compared with independent measurements by R. Giauque using the X-ray fluorescence system described in Ref. 6 which has been accurately calibrated, and its results verified using atomic absorption and neutron activation for many samples including air filters. The agreement between the data is particularly impressive when one

considers that the whole analysis time in the EPA system was only six minutes including data acquisition, spectrum analysis and teletype output.

Based upon the analysis of these and other samples, the variance in a series of measurements in which the errors due to counting statistics can be made arbitrarily small is better than 10%. The accuracy of results for complex analysis is limited mostly by the sophistication of the computer analysis program and the degree of ingenuity used in its application. However, it is safe to say that overall rms errors less than 20% can be easily achieved for most elements.

Similar data have been obtained for the Cu and Tb fluorescers. In each of these cases the multielement interference problems are smaller for most samples relative to Mo excitation. For the higher Z elements, the accuracy is limited mostly by counting statistics in the peak due to the less abundant heavy elements. For the Cu fluorescer, the absorption of low energy X-rays by the sample limits the accuracy. These effects are discussed in more detail in a later section.

TABLE 6. Comparison of Results Obtained on Several Filter Samples[a)]

SAMPLE NUMBER		1	2	3	4	5	6	7	8
Ca	(i)	261 ±17	328 ±18	333 ±18	343 ±18	298 ±18	236 ±17	199 ±16	435 ±20
	(ii)	271 ±25	393 ±25	361 ±25	383 ±44	286 ±45	200 ±43	177 ±42	523 ±52
Ti	(i)	30 ± 7	43 ±12	35 ±10	38 ±12	27 ± 9	16 ± 6	19 ± 6	41 ±12
	(ii)	37 ±18	47 ±20	48 ±10	49 ±20	42 ±15	62 ±20	43 ±15	66 ±15
Mn	(i)	<5	7 ± 5	2 ± 5	26 ± 5	8 ± 5	<5	<5	22 ± 5
	(ii)	11 ± 4	6 ± 4	15 ± 4	27 ± 8	<23	<22	<22	27 ± 8
Fe	(i)	410 ± 8	463 ± 8	421 ± 8	575 ± 8	319 ± 7	212 ± 6	180 ± 6	501 ± 8
	(ii)	405 ±20	466 ±23	421 ±21	572 ±23	371 ±15	243 ±10	180 ± 9	480 ±19
Ni	(i)	8 ± 3	5 ± 3	<3	<3	<3	<3	<3	8 ± 3
	(ii)	4 ± 2	8 ± 2	<6	<11	<11	<11	<11	9 ± 4
Cu	(i)	97 ± 4	74 ± 4	83 ± 4	26 ± 3	4 ± 3	<3	<3	12 ± 3
	(ii)	81 ± 4	53 ± 3	55 ± 3	27 ± 4	7 ± 4	6 ± 4	6 ± 4	18 ± 4
Zn	(i)	59 ± 3	52 ± 3	43 ± 3	111 ± 3	23 ± 3	13 ± 3	10 ± 3	46 ± 3
	(ii)	58 ± 3	51 ± 3	41 ± 2	91 ± 4	24 ± 3	13 ± 3	12 ± 3	40 ± 3
Br	(i)	81 ± 3	157 ± 3	111 ± 3	170 ± 3	174 ± 3	129 ± 3	47 ± 3	394 ± 4
	(ii)	95 ± 5	175 ± 9	127 ± 5	171 ± 7	179 ± 7	129 ± 5	40 ± 4	408 ±16
Pb	(i)	354 ± 8	680 ± 8	451 ± 8	763 ± 9	665 ± 8	511 ± 8	198 ± 6	1329 ±11
	(ii)	327 ±16	716 ±36	449 ±22	747 ±30	702 ±28	563 ±23	196 ± 8	1320 ±53

a) Errors reflect counting statistics only. In case where the quoted error is less than 10%, a 10% calibration error should be assumed.

i) Values measured on EPA system.

ii) Values measured by R. Giauque.

B. Sensitivity

There are a number of ways to express the trace-element detection limit of an analytical method. The usual convention is to define the lower limit of detectability as the amount of an element required to produce a signal equal to the 3σ fluctuation in background under a peak. However, in order to be meaningful, this number must include a specification of the counting interval, and the total size of the sample analyzed. Perhaps most important, these limits should represent experimental measurements on realistic samples and not extrapolations based upon idealized conditions.

Figures 11 and 12 are two logarithmic plots of X-ray fluorescence spectra taken on the same air filter using the Cu and Mo fluorescer. (Similar data were acquired with the Tb fluorescer but are not shown here since a small Ba peak was the only observed elemental line). Each spectrum was acquired in a five minute counting interval; the area of the filter analyzed was 7 cm^2. Typical concentrations are Pb - 1.32 $\mu g/cm^2$, Fe - 0.5 $\mu g/cm^2$, Mn - 30 ng/cm^2, Ca - 0.5 $\mu g/cm^2$. Counting rates were 10 K/sec for Mo, 5 K/sec for Cu. The background beneath the peaks is associated with the coherent/incoherent scatter peaks which are produced by air scatter and by scatter from the 5 ng/cm^2 Millipore filter substrate. (A better peak/background results from operating in a He atmosphere, since, in the case of Mo excitation, 2/3 of the scattering is from the air surrounding this sample.)

Using these data, together with the air sampler calibration data, we calculate the sensitivity vs. Z curves given in Figure 13. These numbers represent the minimum detectable limit (3σ above background) expressed as ng/m^3 in a two hour air sample which is then analyzed for five minutes in

the X-ray system. (To convert these limits to ng/cm^2 on the Millipore sample multiply by 0.8 m^3/cm^2.) To a first approximation these should correlate with the relative efficiency factors shown in Figure 10. Slight difference in the shape of the curves arises from variations in the shape of the background for a given fluorescer; relative differences from one fluorescer to the next are also affected by the difference in incident X-ray yield for each tube setting. In particular, this largely accounts for the values for detectibility measured for Tb excitation being higher then would be expected on the basis of the calculated sensitivities.

Detectable limits achieved under other running conditions can easily be obtained by scaling the numbers obtained from the above graph. The detectable limits are inversely proportional to the total air flow and to the square root of the counting intervals. The background for Millipore and Nucleopore filters are similar whereas the backgrounds from Whatman 41 filters are about four times larger.

An important consideration in comparing these detectable limits with results obtained for competing methods is the multiple-element detection capability of energy dispersive X-ray fluorescence. The three curve segments in Figure 13 represents the sensitivities for <u>simultaneous</u> detection of many elements excited with each of the three fluorescers. (This statement is not rigorously accurate since it neglects reduction in detectibility due to inter-element interferences; however, in cases where the variation in concentration between adjacent elements is not large, the data are accurate enough for comparison.) It can be argued that the sensitivity could be optimized for one element, by filtering the X-rays. However, one of the greatest strengths of the energy dispersive method is its multiple-element capability which would

appear to be important in environmental research and monitoring. Any cost analysis of competing analytical methods should bear this in mind.

C. Particle Size and Matrix Effects

As noted earlier, calibration problems arise for light elements due to the absorption of the very low-energy characteristic X-rays either by the filter matrix or by the individual aerosol particles. Since the mean absorption length for these X-rays may be short compared to particle diameters, or to the filter thickness, the X-ray intensity reaching the detector depends upon the microscopic location from which the X-ray is generated either within the particle or in the filter matrix. Calculations of elemental concentrations using the observed X-ray intensity must then include a correction for this effect.

To calculate a reasonable correction factor, it is necessary to know something about the particle size distribution and the location of the intercepted particles within the filter material. Information concerning particle size must be obtained either by restricting the size range reaching the filter (via impactors for instance), or by making some assumptions regarding the size distribution in the original aerosols. Similarily, the absorption correction due to the filter matrix must be estimated by assuming localization of the particles in the filter, most likely on its surface.

At the best any assumption appears to have dubious merit, so we have limited our investigation of the problem to estimating the maximum effect anticipated in certain limiting cases. This has been done by calculating the difference between the observed X-ray intensity with and without the

absorption effects. Referring to Figure 9 we see that the difference between a thin film X-ray intensity and that including the absorption of the X-rays integrated over a thickness d is given by a factor

$$A = \frac{1 - e^{-(\mu_0 + \mu_1)\rho d}}{(\mu_0 + \mu_1)\,\rho d} \qquad (3)$$

where μ_0 and μ_1 are the total absorption coefficient for the exciting and emitted radiation respectively. If we now associate d with the diameter of a homogeneous particle, we can calculate the absorption correction A as a function of particle size. (This calculation will overestimate the correction for spherical particles since it assumes a constant thickness; however, since so little is known about particle shapes the assumption is as valid as any other.) Figures 14, 15 and 16 are the results of calculations for the case of Al, S and Ca X-rays excited by Cu Kα radiation. The individual curves represent various assumptions regarding particle composition; the hydrocarbon assumes a unit density material having the absorption cross sections of carbon. The results indicate that no serious problems occur for particles of size below 10 μ except in the case of Al. Estimates of matrix effects can also be obtained from these curves by recognizing that the 5 ng/cm^2 Millipore filter is equivalent to a 50 μ thick hydrocarbon sample. Thus, if the material were uniformly distributed throughout the filter, the correction to the intensity at its maximum would be the value of the hydrocarbon absorption correction at 50 μ. Again the correction is not too serious except in the case of Al.

These families of curves represent a guess as to likely chemical constituents of particles. It is possible that more difficult combinations of elements might produce significant absorption effects (PbS is an obvious candidate). Again we are faced with the necessity of making some assumptions regarding the nature of particulates in order to estimate the correction factor.

The problems associated with these effects are of course inherent to the X-ray fluorescence method and are the same regardless of how one excites or detects the radiation. However, additional information can be obtained by using a monoenergetic X-ray source to generate the characteristic radiation. As noted in Eq. 3, the correction factor depends upon the absorption coefficient for both the incident and emitted X-rays. By varying the incident X-ray energy, two measurements can be performed, one in which absorption of the incident radiation is neglible over the particle diameter, and the other where it is significant. Another way of looking at the problem is to consider the higher energy excitation as a probe measuring the total particle volume, whereas the low-energy excitation samples the surface only. In this way information regarding the absorption characteristics of the particle can be obtained. To a first approximation, this measured absorption correction would be independent of any assumptions regarding particle shape or composition. A similar arguement could be applied to the question of matrix absorption within the filter.

6. CONCLUSIONS

The EPA X-ray fluorescence analyzer is now a complete engineered system, and our tests indicate that it is capable of processing large numbers of air filters with adequate accuracy for this application. Some of the experimental studies discussed in this report were designed to examine limitations that will require further exploration at EPA in order to extend the applications of the instrument to low-Z elements and samples other than Millipore filters.

REFERENCES

1. C. M. Lederer, J. M. Hollander, I. Perlman, Table of Isotopes 6th Edition, p. 570 (1967) Wiley.

2. D. A. Landis, F. S. Goulding and J. M. Jaklevic, Nucl. Instr. and Methods, 87, 211 (1970).

3. F. S. Goulding, J. M. Jaklevic, B. V. Jarrett and D. A. Landis, Advances in X-ray Analysis, 15, 470 (1972) Plenum Press.

4. W. H. McMaster, N. Kerr Del Grande, J. H. Mallett and J. H. Hubbell, Compilation of X-ray Cross Section, Lawrence Livermore Laboratory Report UCRL-50174.

5. J. S. Hansen, H. V. Freund, R. W. Fink, Nucl. Phys., A142, 604 (1970).

6. R. D. Giauque, F. S. Goulding, J. M. Jaklevic and R. H. Pehl, Trace-element Analysis with Semiconductor Detector X-ray Spectrometers, Lawrence Berkeley Laboratory Report, LBL-647.

TABLES

Page

Table 1. Elements measured by the system and their X-ray absorption and emission energies. 4

Table 2. Reproducibility of areas calculated with computer program. . . 19

Table 3. Computer output of results. 23

Table 4. Comparison of measured concentrations of standard samples. . . . 26

Table 5. Detectability of cobolt as a function of iron concentration. . . 29

Table 6. Comparisons between measurements made on several filters by R. Giauque and using the EPA system. 31

Table A.1 Elements potentially amenable to study A.4

FIGURES

Fig. 1. Calculated relative K X-ray production yields for three excitation energies (Cu Kα, Mo Kα, Tb Kα X-rays). 40

Fig. 2. Schematic diagram of the sampling station. 41

Fig. 3. Resolution vs. energy for various X-ray systems 42

Fig. 4. Efficiency of a 3 mm thick silicon detector as a function of X-ray energy. 43

Fig. 5. Diagram of the geometry used in the final design. 44

Fig. 6. Variation of output counting rate with input rate for various dead times. The last pulses have been rejected by the pile-up rejector. 45

Fig. 7. Illustration of spectrum stripping procedure 46

Fig. 8. A typical K X-ray spectrum due to one element. The regions identified in this figure must be defined during the CALIBRATION phase of set up for the instrument 47

Fig. 9. Expression for the overall efficiency of the process of production, absorption and detection of the fluorescent X-rays 48

Fig. 10. Actual relative efficiency curves for three fluorescers. These can be compared with the theoretical curves of Figure 1. 49

Fig. 11. Air filters spectrum taken using the copper fluorescer. 50

Fig. 12. Air filters spectrum taken using the molybdenum fluorescer. 51

Fig. 13. Elemental detection sensitivity curves for the three fluorescers (two hour sample collection time, five minute analysis time on each fluorescer). 52

Fig. 14. Calcium X-ray attenuation vs. particle size. 53

Fig. 15. Sulphur X-ray attenuation vs. particle size. 54

Fig. 16. Aluminum X-ray attenuation vs. particle size. 55

Fig. A.1 Design of filter carrier A.7

Fig. A.2 Block diagram of spectrometer A.8

Fig. A.3 Estimated elemental abundancies and system sensitivity. (10 min. analysis at 100 μA for each of 3 fluorescers; samples collection at 10 liters/min-cm^2) A.9

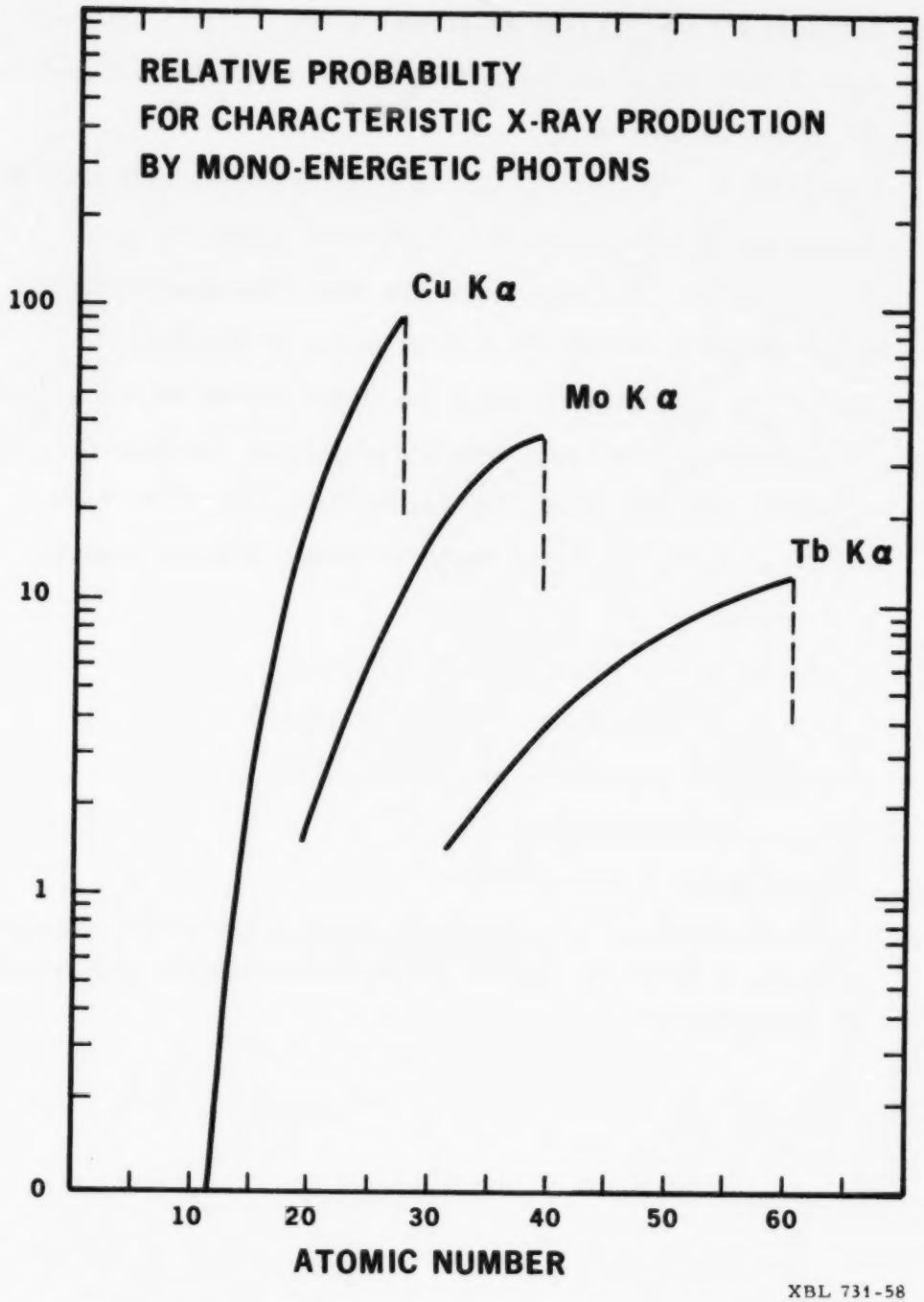

Fig. 1. Calculated relative K X-ray production yields for three excitation energies (Cu Kα, Mo Kα, Tb KαX-rays).

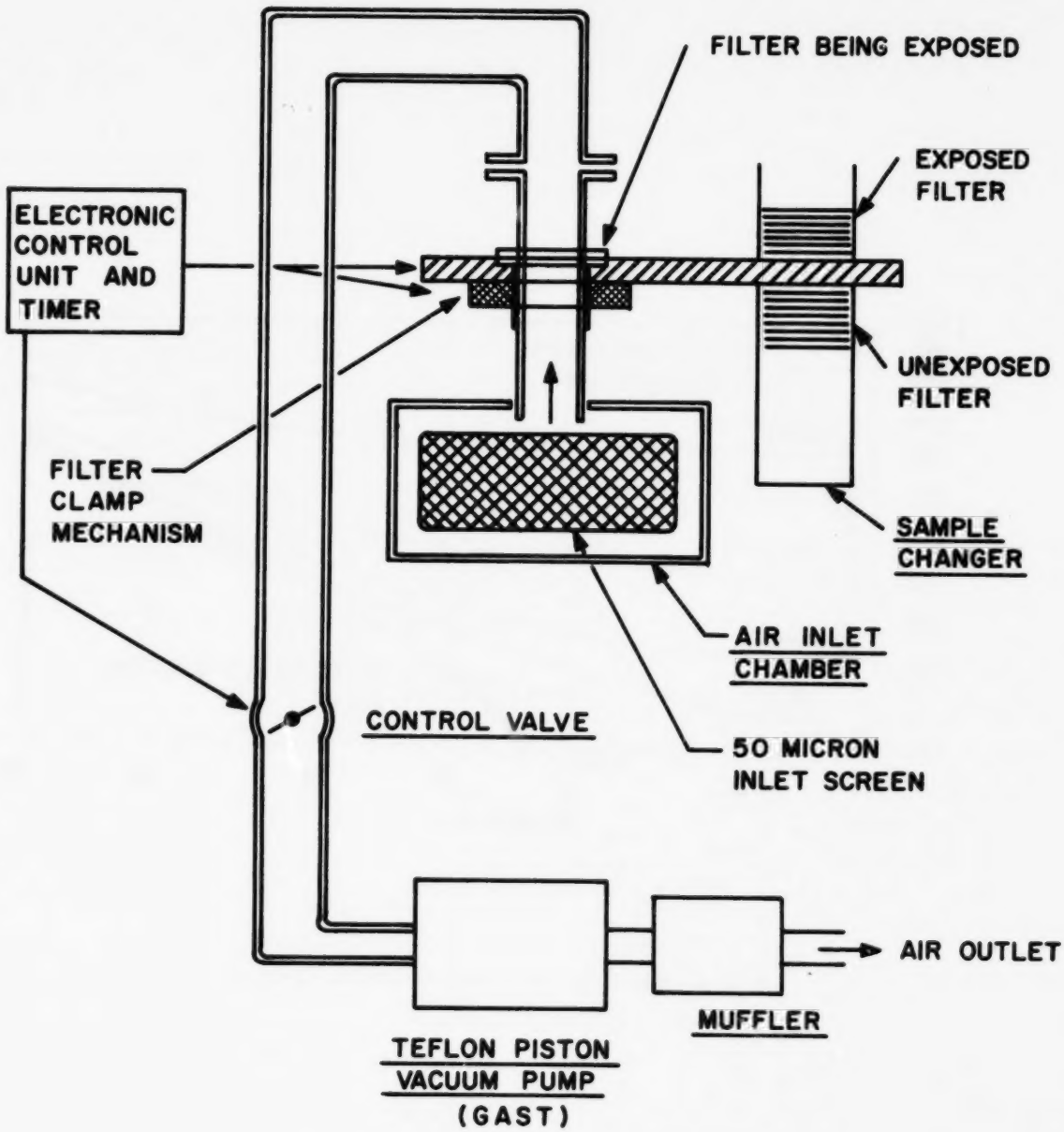

Fig. 2. Schematic diagram of sampling station.

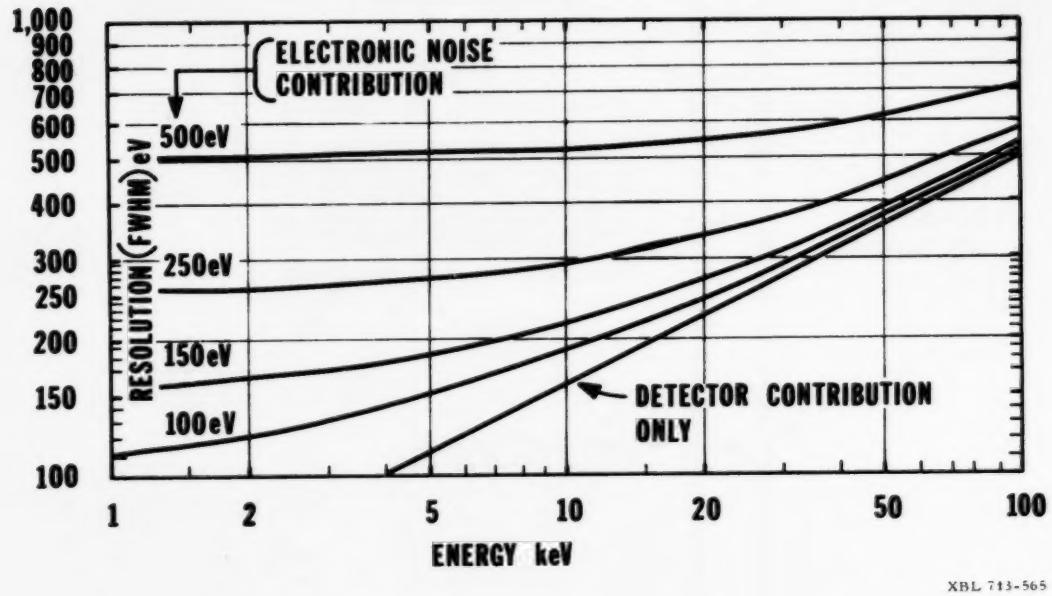

Fig. 3. Resolution vs. energy for various X-ray systems.

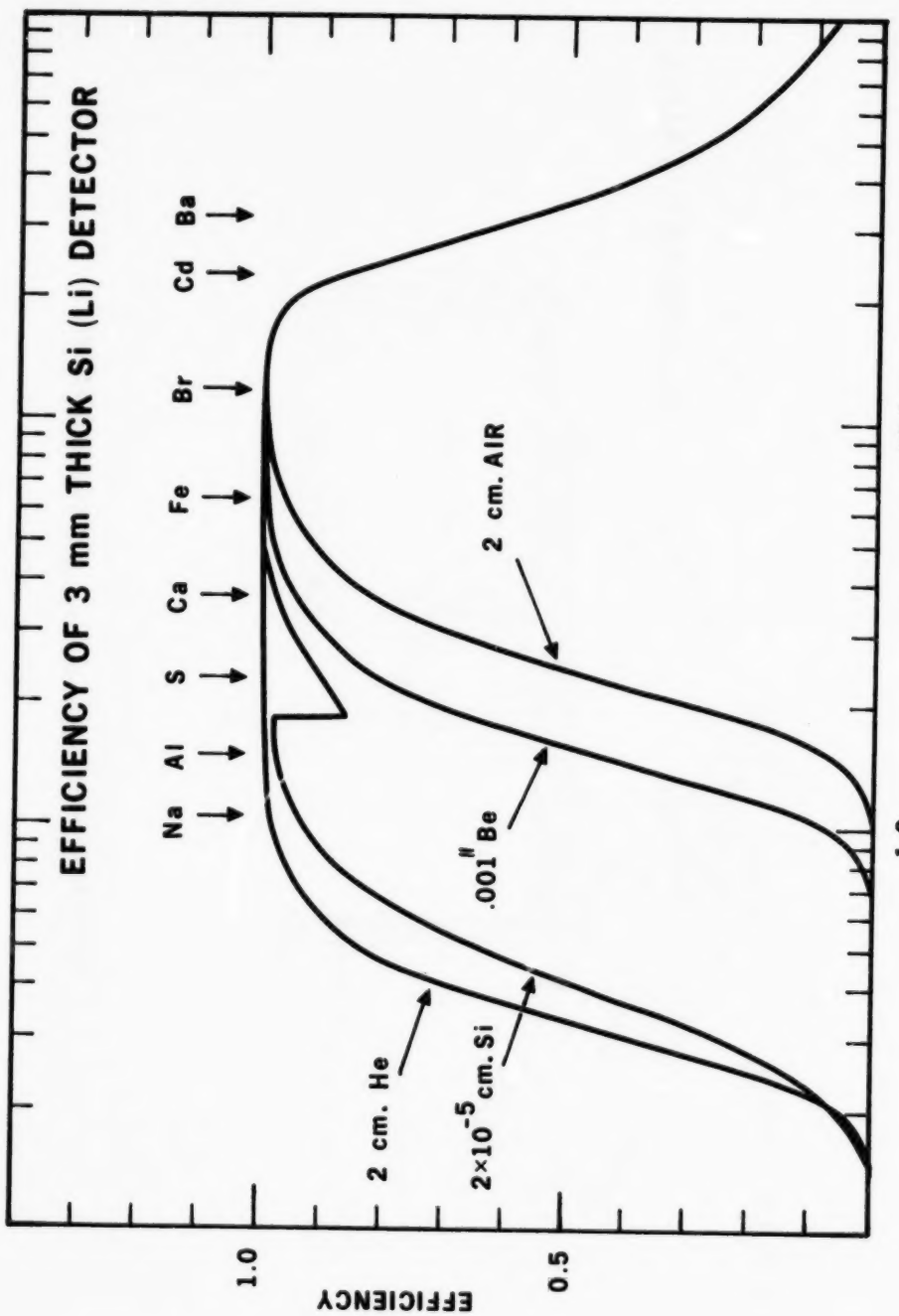

Fig. 4. Efficiency of a 3mm thick silicon detector as a function of X-ray energy.

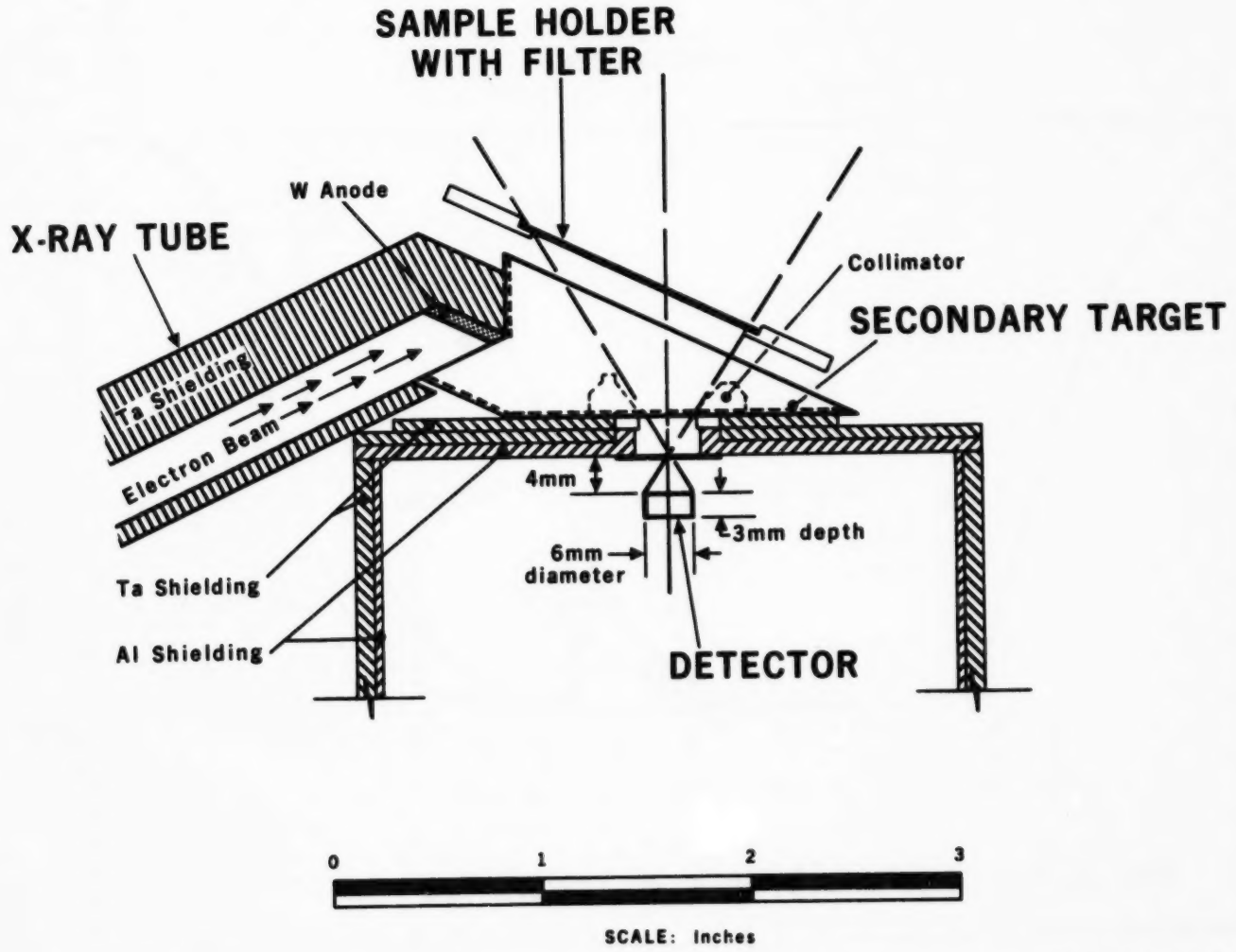

XBL 731-102

Fig. 5. Diagram of the geometry used in the final design.

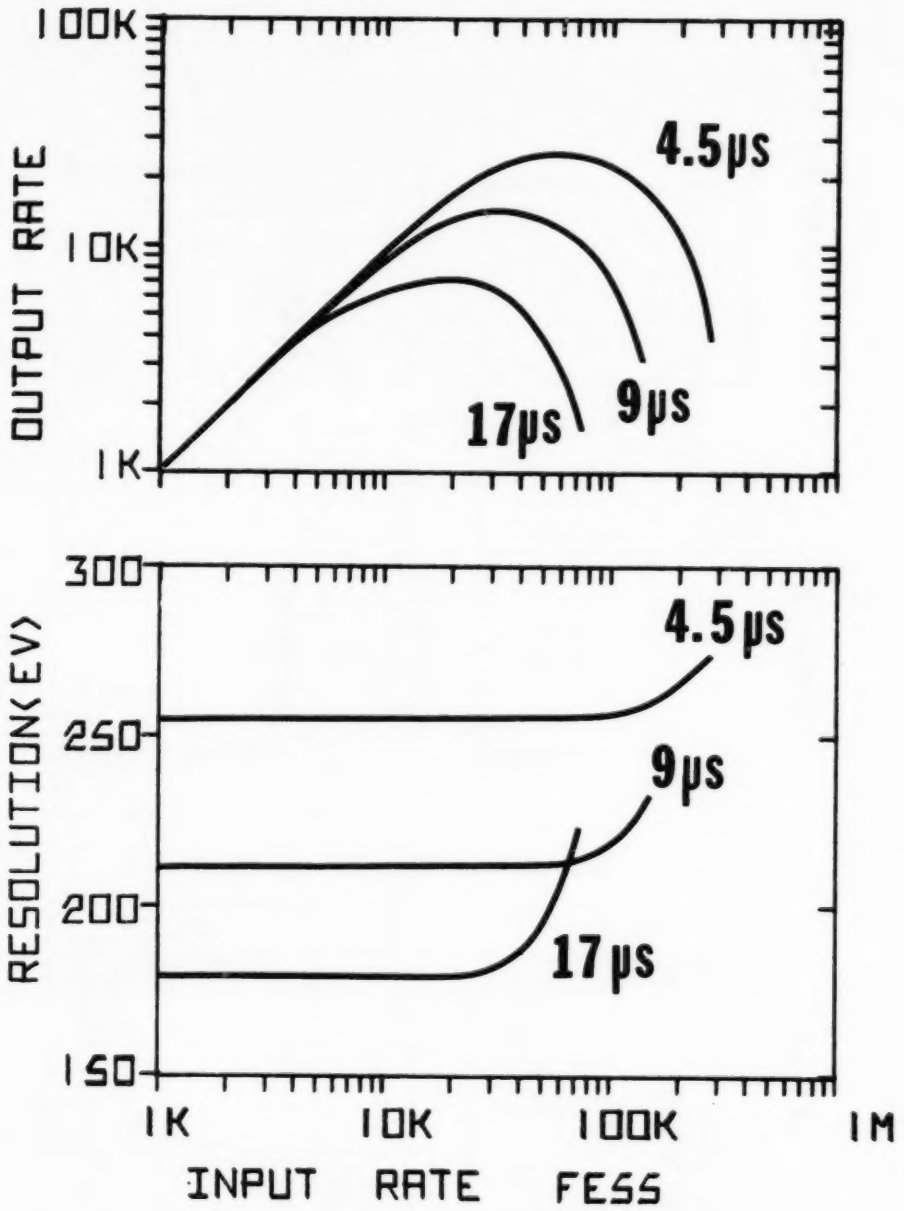

XBL 7010-6806

Fig. 6. Variation of output counting rate with input rate for various dead times. The last pulses have been rejected by the pile-up rejector.

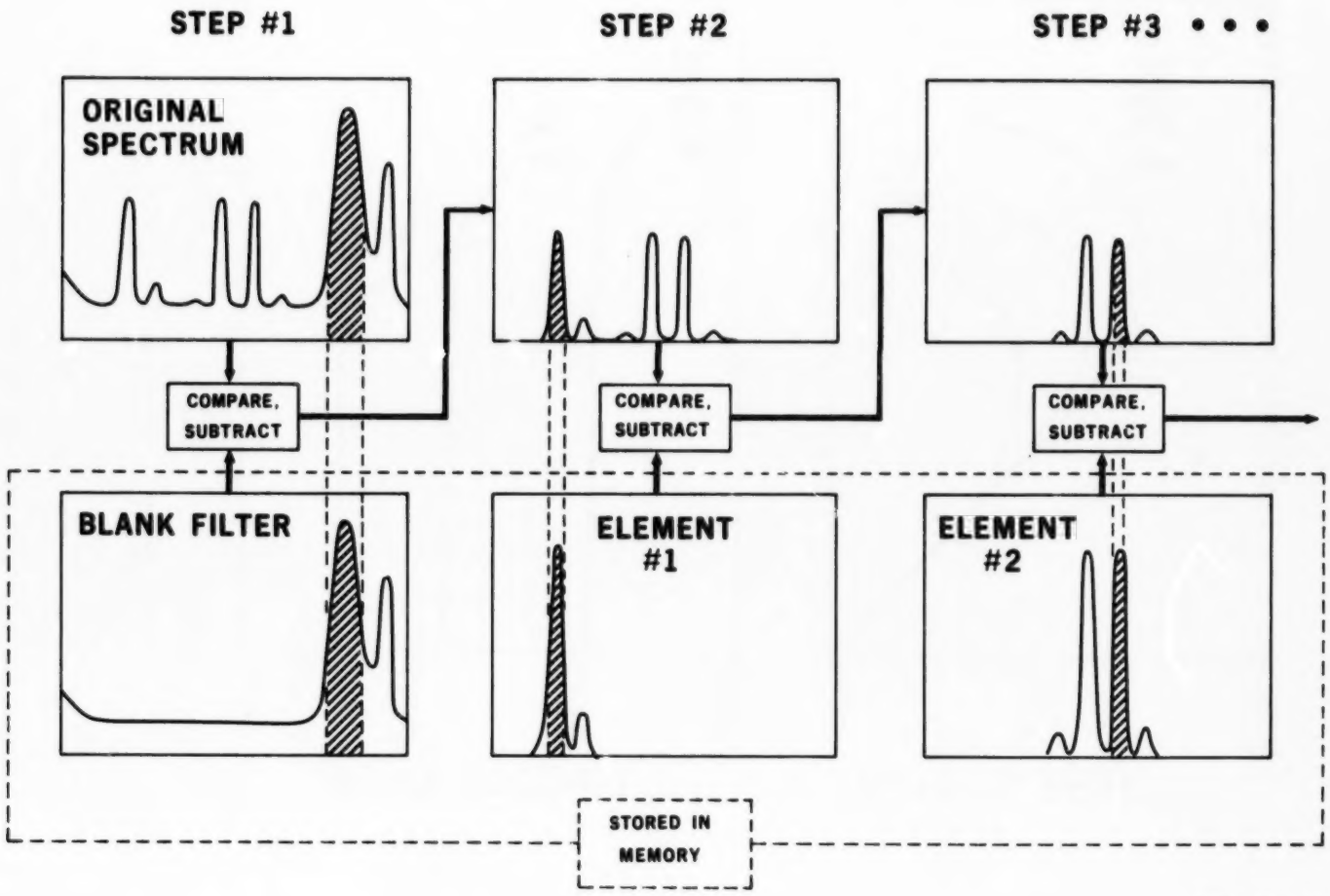

Fig. 7. Illustration of spectrum stripping procedure.

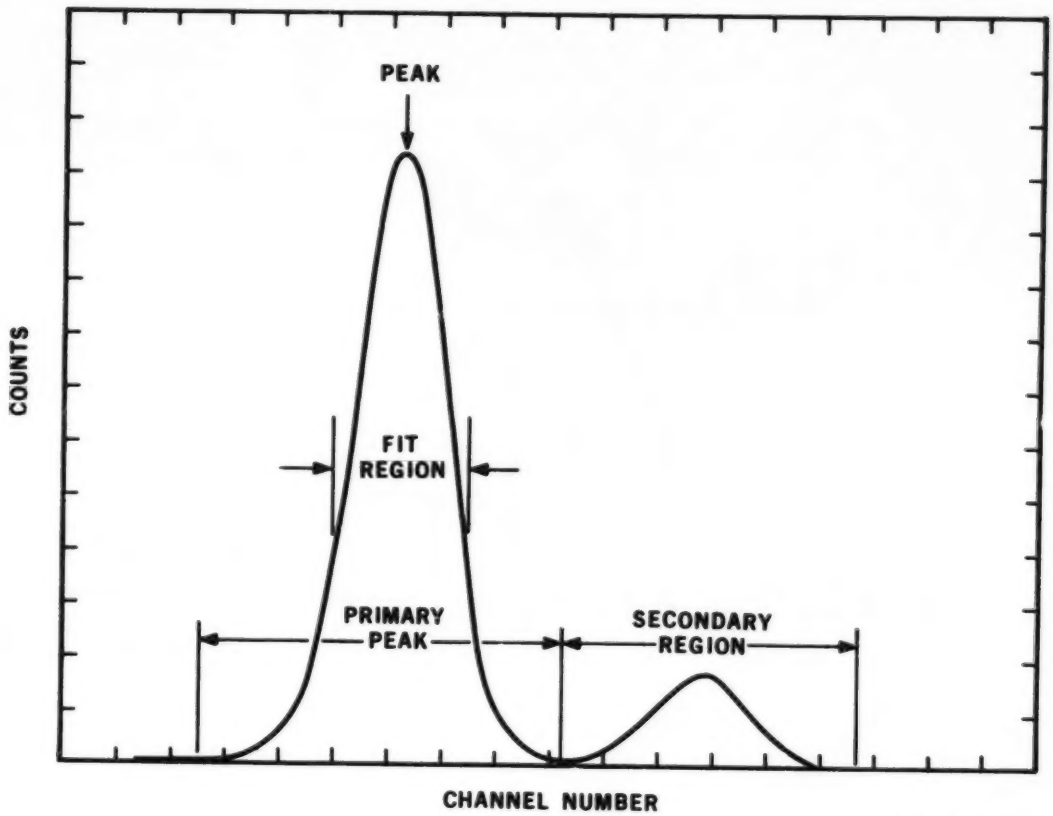

Fig. 8. A typical K X-ray spectrum due to one element. The regions identified in this figure must be defined during the CALIBRATION phase of set up for the instrument.

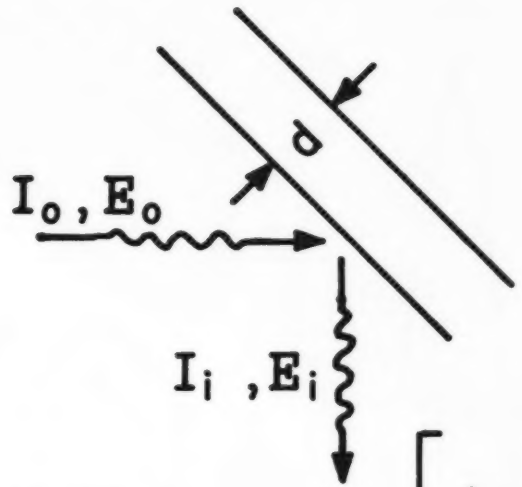

$$I_i = I_o G \rho_i d \tau_i \omega_k^i \epsilon_i \left[\frac{1 - e^{-(\mu_o + \mu_i)\rho d}}{(\mu_o + \mu_i)\rho d} \right]$$

XBL 7110-1500

Fig. 9. Expression for the overall efficiency of the process of production, absorption and detection of the fluorescent X-rays.

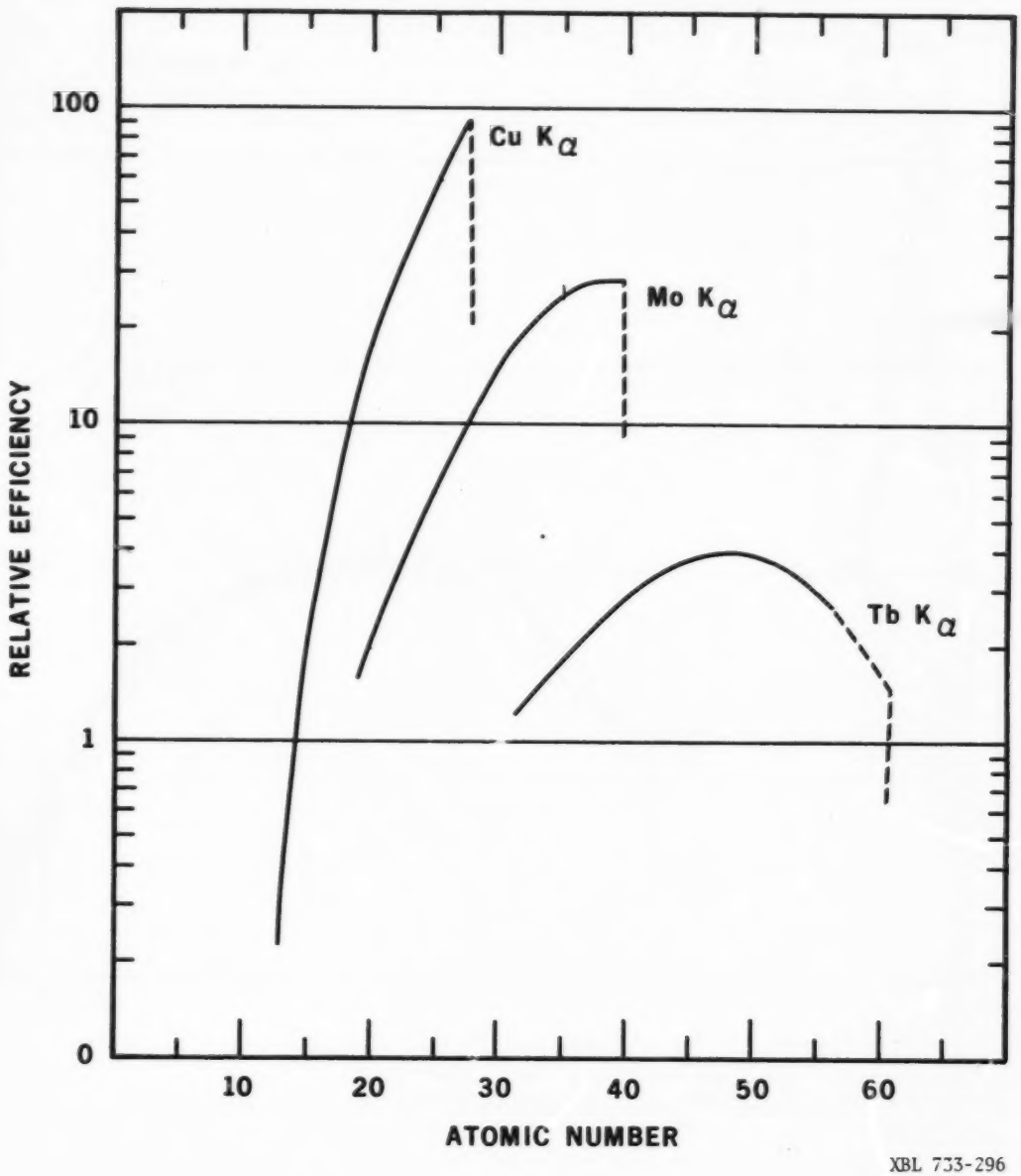

Fig. 10. Actual relative efficiency curves for three fluorescers. These can be compared with the theoretical curves of Figure 1.

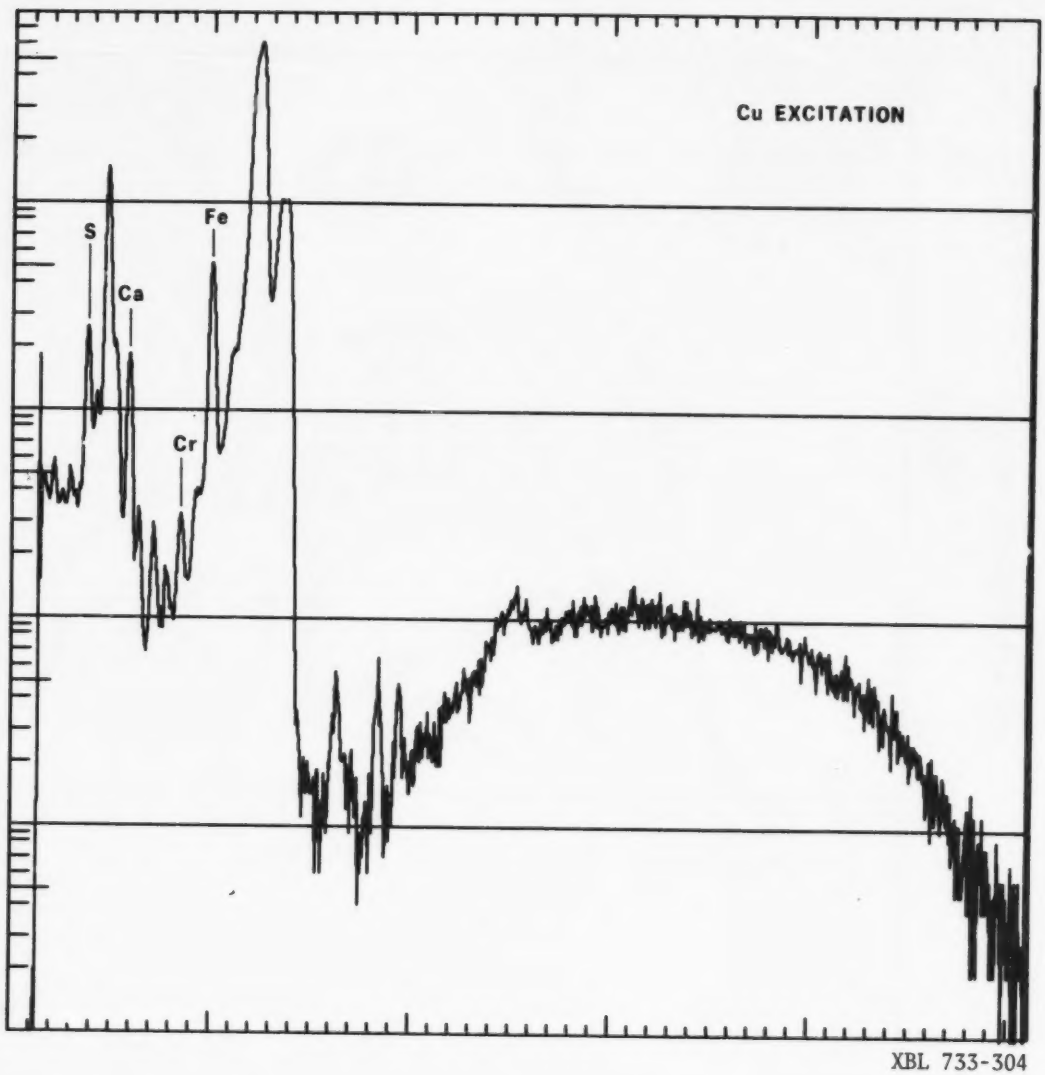

Fig. 11. Air filters spectrum taken using the copper fluorescer.

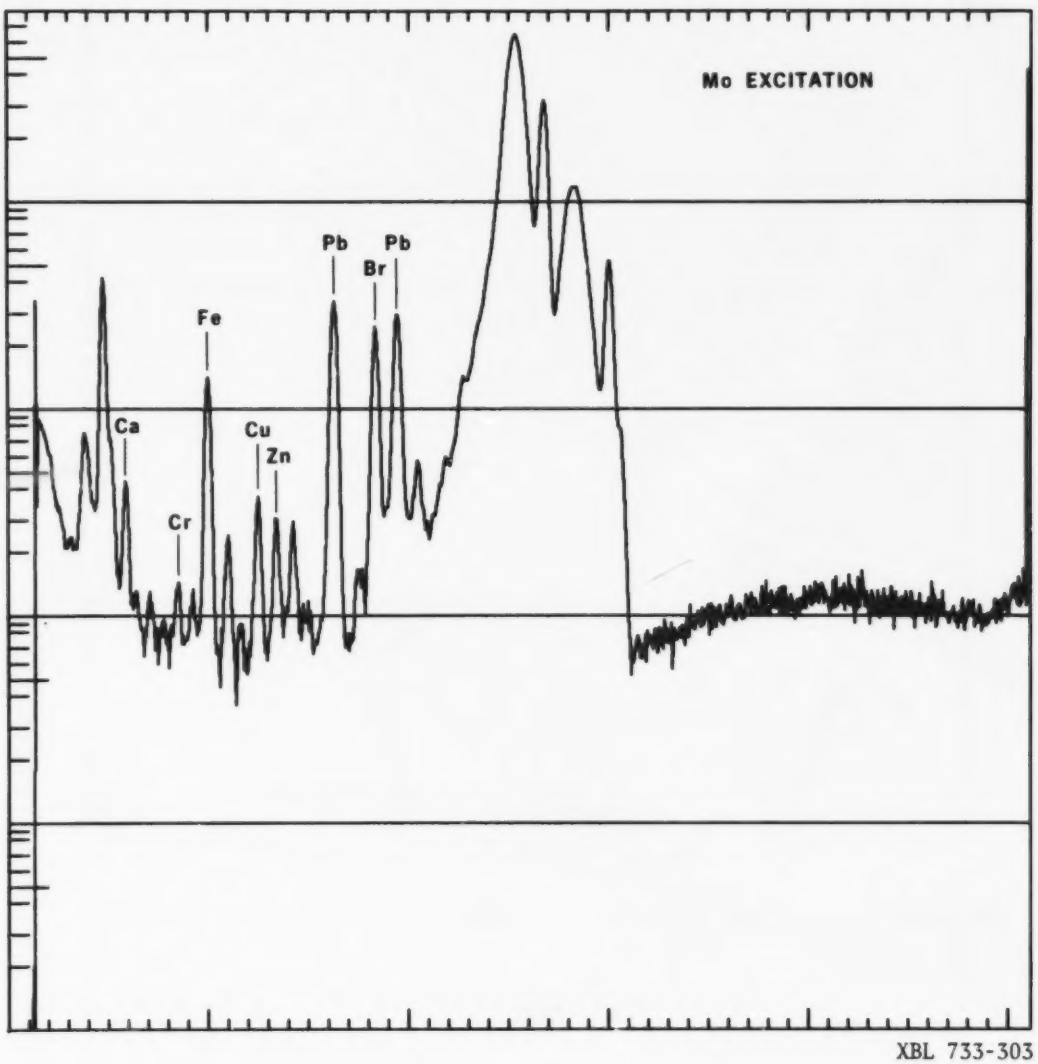

Fig. 12. Air filters spectrum taken using the molybdenum fluorescer.

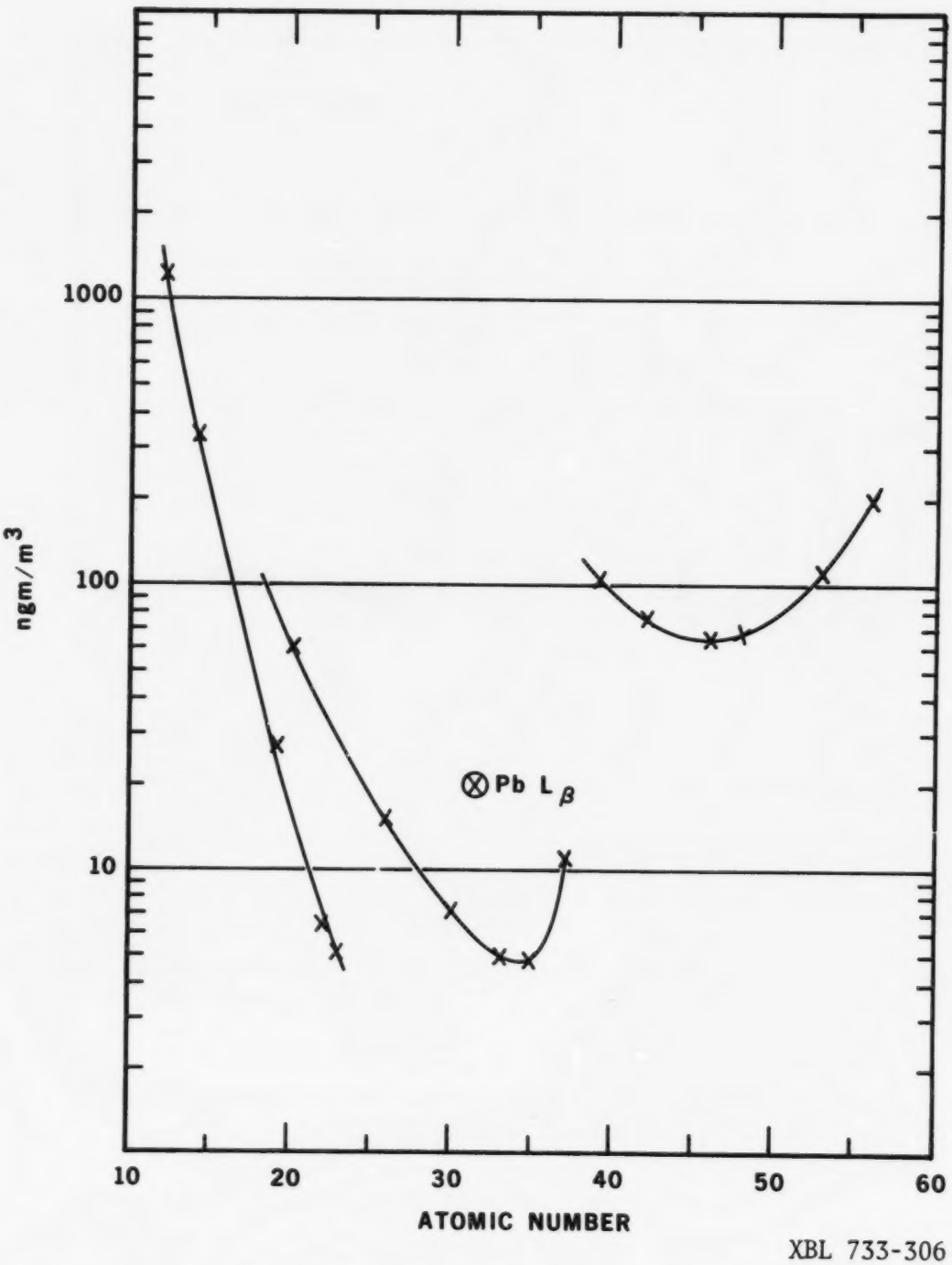

Fig. 13. Elemental detection sensitivity curves for the three fluorescers (two hour sample collection time, five minute analysis time on each fluorescer).

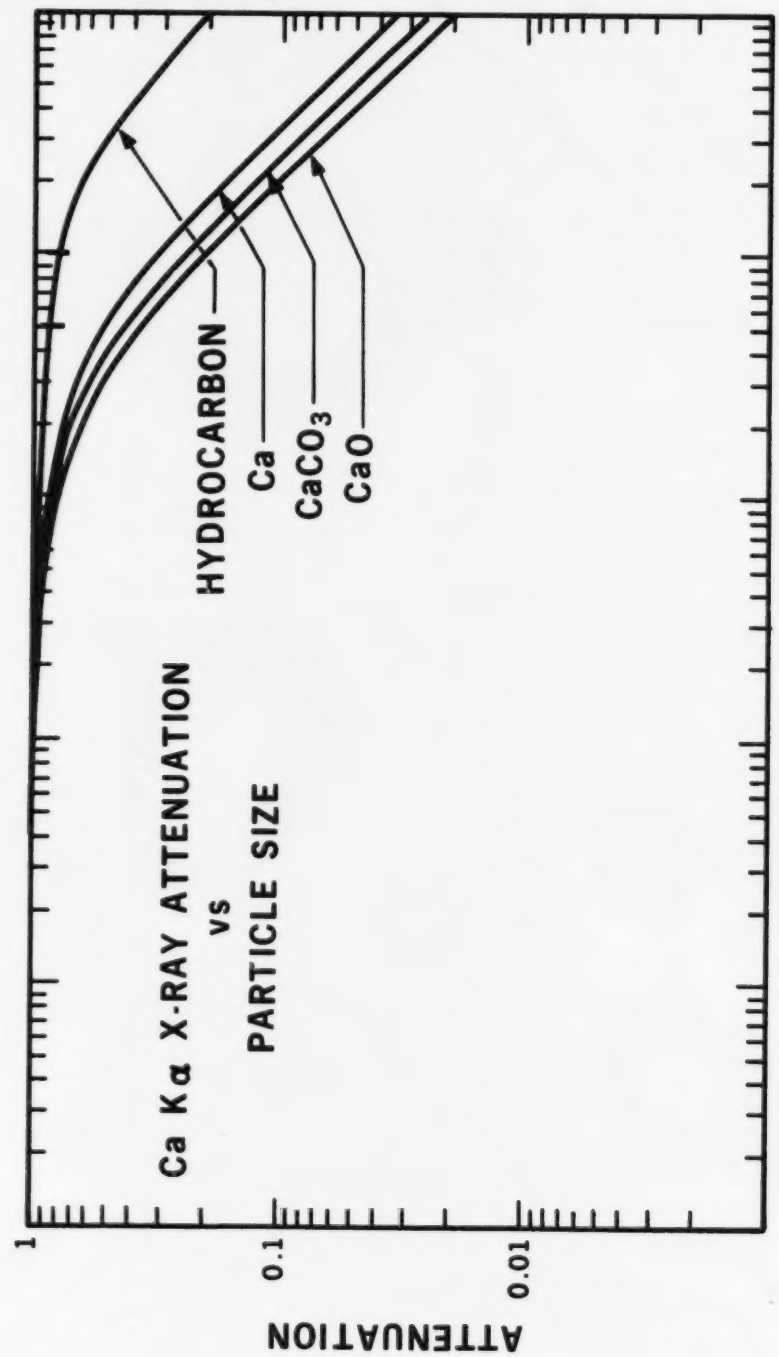

Fig. 14. Calcium X-ray attenuation vs. particle size.

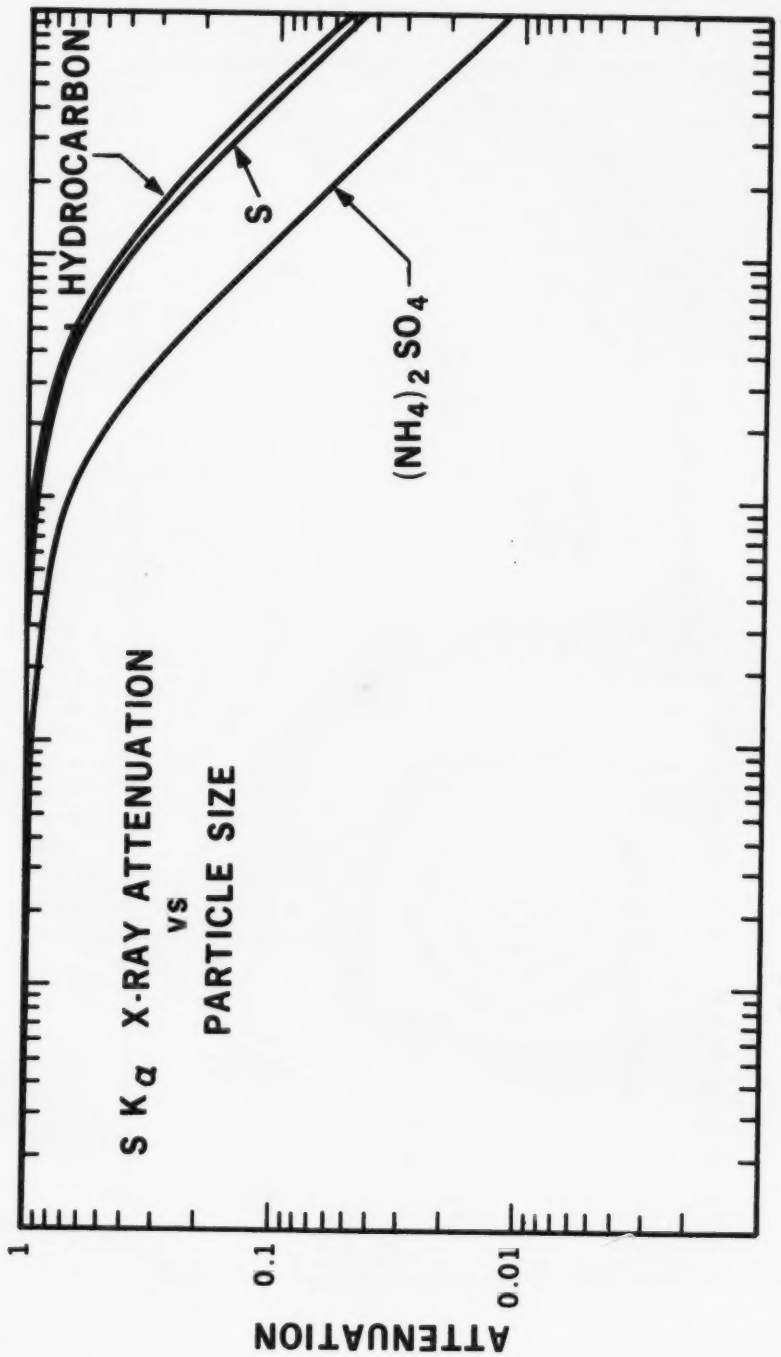

XBL 731-59

Fig. 15. Sulphur X-ray attenuation versus particle size.

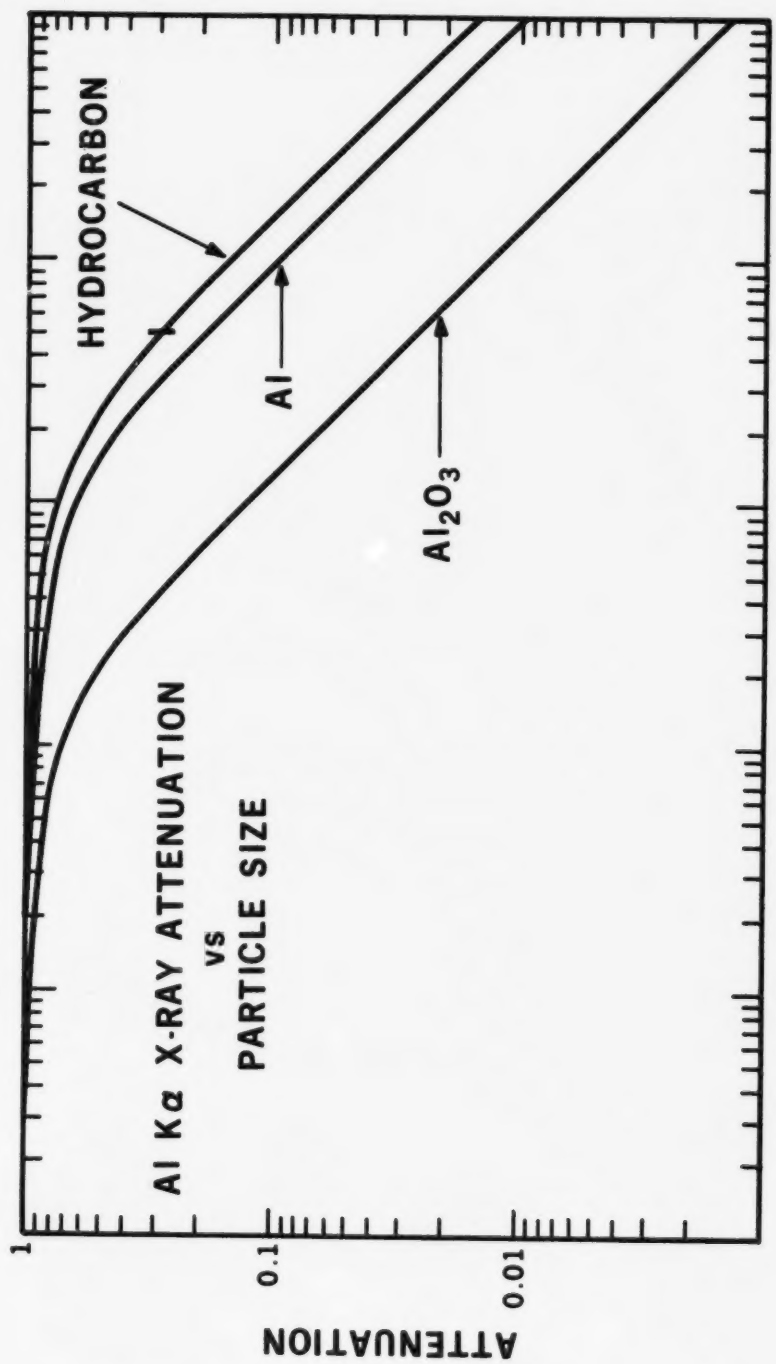

XBL 731-57

Fig. 16. Aluminum X-ray attenuation vs. particle size.

APPENDIX

EXTRACTS FROM FIRST PROGRESS REPORT

MONITORING SYSTEM DESIGN

As the design of hardware must conform to the whole monitoring system parameters, it is essential at the outset to make decisions on the overall system. The following factors enter into these decisions:

A. Filter Specification and Logistics

As shown in our earlier work on X-ray fluorescence analysis, the principal background observed in X-ray fluorescence spectra is produced by scatter of the primary radiation from the matrix of the sample into the detector. It is therefore essential to use low-mass filters containing only very light elements. Furthermore, the filter should be virtually free of elemental contaminants in the range of elements to be investigated (i.e. approximately from sulphur to barium in the periodic table, and also the heavy elements).

The ideal X-ray spectrometer geometry examines an area about 1 inch in diameter on a filter. Therefore there is no reason to use filters much larger than this. To avoid the possibility of wall effects in the sampling pipe producing a serious non-uniformity over the area examined, we have chosen to use filters 37 mm in diameter. Such filters can be obtained from Millipore, Gelman and Nucleopore at prices near $200/1000. Results obtained in our laboratory and by other workers indicate that these filters satisfy the general requirements for X-ray analysis. The availability of several types of filter in this size will facilitate intercomparisons between their properties at a later date.

The handling of large numbers of filters can only conveniently be accomplished by mounting filters on a suitable carrier, which must cost significantly less than the filter itself. Furthermore, the carrier should be of such a size as to utilize convenient means of storage. Plastic mouldings offer the prospect of meeting these requirements at minimum cost. The design chosen for the carrier is shown in Figure A.1; its overall dimensions are 2" square (suitable for storage in common 35 mm slide-boxes), with provision for mounting filters into the 37 mm diameter recess. Keying is provided for orientation of the filter at one corner and a recessed shelf at one edge provides a suitable area for identification markings (either manual or automatic). The design allows for automated manipulation of the carriers both at the air sampler, and at the analysis facility.

Preliminary estimates for the moulding costs have been obtained; it appears likely that the carriers will cost about 5¢ each in 10,000 quantities after the first order. Initial tooling will cost approximately $2000--this cost will be borne by the first order for 10,000 units.

B. Scope of System: Number of Filters and Elements for Analysis

The complexity of the data-processing requirements, and the need for automatic sample handling, is determined by the range of elements to be studied, and by the size of the whole monitoring system. After discussions with EPA representatives, and with other authorities, the following targets have been set:

i) A typical monitoring complex might consist of ten sampling stations each producing an average of three filters per day. Unattended, automatic operation of these stations for a week or

more appears desirable. This implies that the design of the sample changer should be suitable for holding at least 21 filters--30 has been chosen as the design objective. If used for daily filter changes, this will permit one month of unattended operation. One of our objectives will also be to use components (e.g. vacuum pump) requiring routine attention no more frequently than once a month.

ii) An analysis station must be capable of handling the analysis of over 30 filters per day produced by the ten sampling stations. Our design objective is 50 filters per day. By allowing 30 minutes analysis time per filter, and by providing automatic operation on a 24 hour per day basis, we will be able to achieve this objective. Our experience has shown that coverage of the range of elements of interest requires X-ray analysis with three different excitation energies. Therefore the 30 minute analysis time is broken down into three separate time intervals each of ten minutes duration. The excitation X-rays for these intervals will probably be the K radiation of Ni, Mo, and possibly Gd. Using these exciting radiations, the interesting elements shown in Table A.1 are potentially amenable to study. In practice, various effects will limit the sensitivity for some of these elements, but, as one purpose of the contract is to evaluate these limitations, it is essential to provide coverage for the entire range.

Table A.1: Elements Potentially Amenable to Study

Element	Kα Energy	Element	Lα	Lβ	Energies
Al	1.49	W	8.40	9.67	
Si	1.74	Hg	9.95	11.85	
P	2.02	Pb	10.52	12.61	
S	2.31	Bi	10.80	13.00	
Cl	2.62				
K	3.31				
Ca	3.69				
Ti	4.51				
V	4.95				
Cr	5.41				
Mn	5.90				
Fe	6.40				
Co	6.93				
Ni	7.47				
Cu	8.04				
Zn	8.63				
Ga	9.24				
As	10.53				
Se	11.21				
Br	11.91				
Rb	13.38				
Sr	14.14				
Zr	15.75				
Nb	16.58				
Mo	17.44				
Cd	23.11				
In	24.21				
Sn	25.19				
Sb	26.36				
I	28.61				
Ba	32.07				

ANALYSIS STATION

Overall Spectrometer Design

The various components of the spectrometer are shown in the block diagram (Figure A.2). Overall control of the system rests with the T1960A computer. Under program control, this instructs the X-ray spectrometer to change samples, to change fluorescer, to turn on helium flow over the X-ray detector for low-energy measurements, and to start an analysis of a sample. The main sequencer in the spectrometer acts as the interface for these instructions. Control of the X-ray tube anode voltage is also exercised by this unit to provide the optimum anode voltage for excitation of the fluorescer, which, in turn, excites the sample.

The computer also acts as a pulse-height analyzer (together with the 1024-channel Northern Scientific ADC), sorting X-ray pulses derived from the detector-preamplifier-amplifier combination. The counting-time is controlled by a preset timer (operating on live-time and thereby correcting for dead time losses in the system). At the end of the preset counting interval, the main sequencer flags the computer, initiating computer analysis of the accumulated spectrum. The results of the elemental analysis are printed out immediately together with estimated errors. The computer also initiates the required actions in the spectrometer preparatory to the next counting interval.

A monitor is provided on the liquid nitrogen level in its storage dewar; if the level falls below the five day reserve level (normal capacity ~40 days), a flashing indicator shows this, and computer printouts will warn the operator until the condition is corrected.

Filament power and high-voltage for the X-ray tube are supplied by a high-voltage power supply which provides accurate and stable voltages under servo control.

Peripheral equipment, to be supplied with the computer, includes a display, a teletype (including tape-reader) that prints all analysis results, a magnetic tape used for program storage and data output, and a "program switch panel". The design of this panel will permit the operator to select and initiate several standard routines without requiring any familiarity with the computer system.

Early work indicates that a detection limit better than 10 ng/cm^2 can be achieved for most elements. For an MF Millipore 0.8 μpore size filter, flow rate at 70 cm Hg pressure equals 10 l/min/cm^2, in two hours, total volume equals 1.2 m^3/cm^2 of filter. Therefore, detection limit ≈ 10 ng/m^3 of air. This quantity is inversely proportional to the sample collection time, and is inversely proportional to (analysis time)$^{1/2}$. While the 10 l/min/cm^2 is probably a somewhat higher airflow than we will use, it is a convenient figure to use for this calculation.

It is of considerable interest to ascertain the elements likely to be observed in air filters with these detection sensitivities. Figure A.3 presents data on this question. The anticipated levels of elements indicated in this figure represent best guesses based on very sparse data in the literature. Those elements where special problems occur with X-ray analysis are so indicated. From this figure, we can guess that a two hour sample will reveal between 15 and 25 elements; an eight hour sample, 20 to 25; and a 24 hour sample, over 25 elements. As the levels indicated for most of the elements in this figure are their normal range, large increases above normal will be measureable for virtually any of the 35 elements shown here.

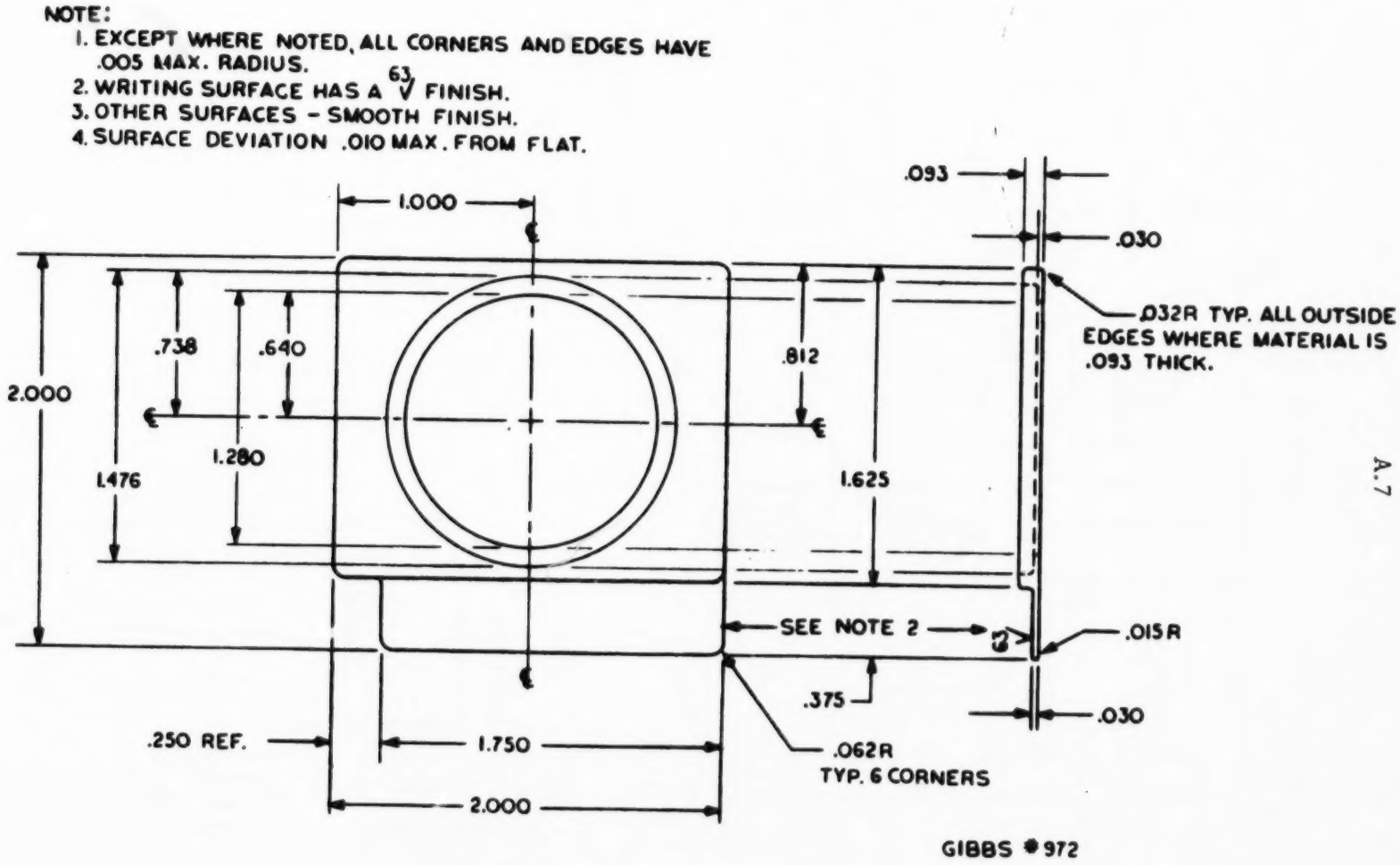

Fig. A.1. Design of filter carrier.

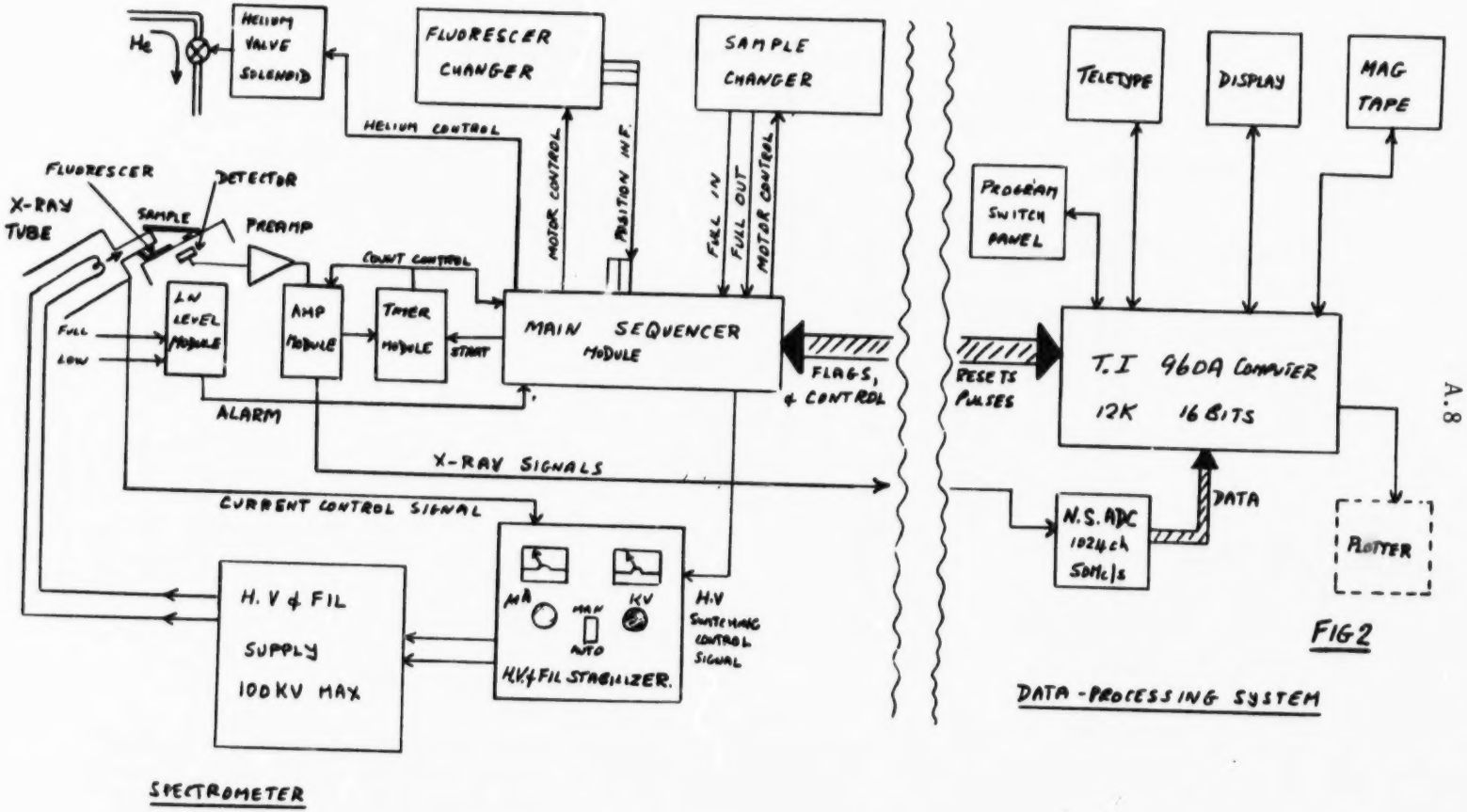

FIG 2

A.8

Fig. A.2. Block diagram of spectrometer.

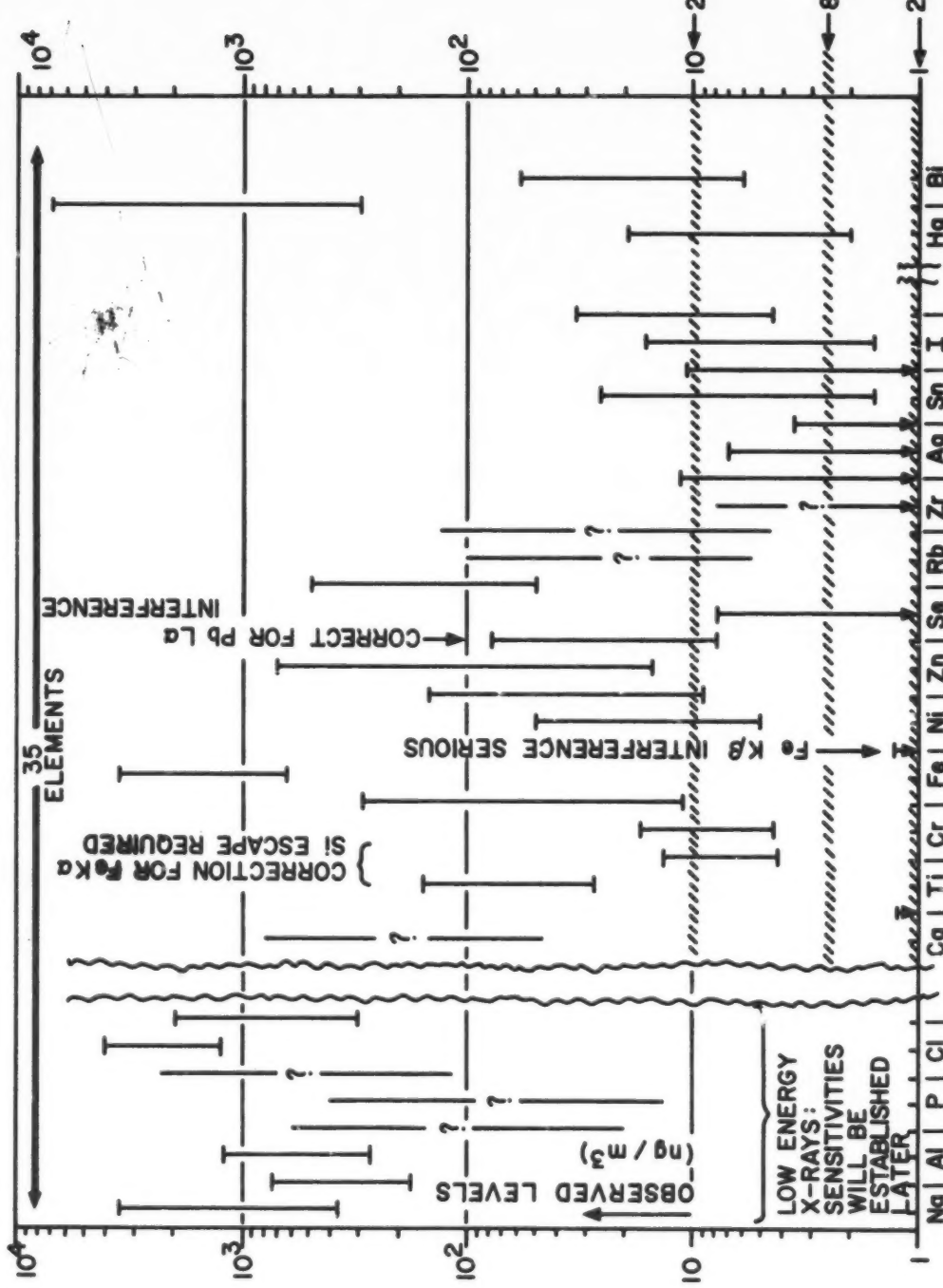
APPROX. DETECTION LIMITS FOR VARIOUS SAMPLING TIMES
2hr
8hr
24hr
35 ELEMENTS
CORRECT FOR Pb Lα INTERFERENCE
CORRECTION FOR FeKα Si ESCAPE REQUIRED
Fe Kβ INTERFERENCE SERIOUS
OBSERVED LEVELS (ng / m3)
LOW ENERGY X-RAYS: SENSITIVITIES WILL BE ESTABLISHED LATER
Na Al P Cl Mg Si S K Ca Ti Cr Fe Sc V Mn Co Ni Cu Zn As Se Br Rb Sr Zr Mo Ag Cd Sn Sb I Ba Hg Bi Pb

Fig. A.3. Estimated elemental abundancies and system sensitivity. (10 min. analysis at 100μA for each of 3 fluorescers; samples collection at 10 liters/min-cm2).